CONCEPTUAL DESIGN REVIEW

Oculus Superne – Team 2
AAE 451, Spring 2007

Design Team

Andrew Cottle	Brian Roth
Sean Duncan	Dave Stinson
Lin Haack	Jeff Studtman
Afzaal Hassan	Justin Wheeler

April 26, 2007

Executive Summary

Oculus Superne is currently designing an UAS to perform extensive land and structure observations. The UAS completes three separate missions: pipeline surveillance, power line surveillance, and forest monitoring. The line-surveying mission provides the customer with the capability to monitor broad tracts of pipe or power line systems for leaks or damage, to provide rapid alerts if detected, and to provide the capability for extended loiter to monitor a damaged segment. The leaks or damages result from natural disasters, accidents, or unauthorized third-party encroachment.

A payload package consisting of LIDAR and an IR/visual camera facilitates the mission. The LIDAR scans for geographic shifts in areas surrounding the lines and performs vegetation surveys. The IR/visual camera combination aids in monitoring for third-part encroachment, physical damage and in navigation. The total package weighs approximately 60 pounds installed and draws 155W (.21 hp) in operation.

The propulsion system, based on initial sizing estimates, is a 40hp off the shelf rotary engine. With engine fixed and the payload weight held constant, trade studies show that the optimal aspect ratio and wing loading are 10 and 20.3 (lbs/ft^2) respectively. The ACS sizing code output gives a gross takeoff weight of 255 pounds, an endurance of 14.38 hours, a lift to drag ratio of 13, and a range of 1300 nautical miles for the UAV. It has a cruise velocity of 100 knots, at an altitude of 5000 feet above see level. A short take off distance of 915 feet, a landing distance of 537 feet and a power to weight ratio of 0.15 horsepower per pound, the pusher prop UAV can take off and land from rough airfields.

The average total cost of a package including ground station, relay station and UAV is $62,600 per system, which does not include the cost of the sensor package. This sets the break-even point for Oculus Superne at 80 systems over a period of 5 years. The average projected cost of operation is $154,000 a year for the customer.

Table of Contents

List of Figures

List of Tables

1 Introduction

The unmanned aerial vehicle (UAV) has made its way quickly and decisively to the forefront of aviation technology. Opportunities exist in a broadening number of fields for the application of UAV systems as the components of these systems become increasingly lighter and powerful. Of particular interest are those occupations that require the execution of missions that depend heavily on dull, dirty, or dangerous work (often referred to as "3-D missions"). UAVs provide a cheap, safe alternative to manned systems and often provide a far greater magnitude of capability.

The mission of the system designed in this report is that of continuous area coverage. The applications for reliable, inexpensive and long-endurance coverage for a particular region are broad and varied. Many of the capabilities offered by a low-cost, high-endurance platform are currently unattainable with manned systems such as helicopters providing rudimentary services. The problem is, therefore, to produce a conceptual design and develop that outline into a preliminary design model to fulfill this continuous area coverage requirement to a degree that would appeal to the target market.

1.1 Mission Overview

The mission of Oculus Superne is to provide a multi-service UAS (Unmanned Aerial System) which acts as the primary detection method for third party infringement of pipelines, performs power-line equipment inspection, detects threats to forested areas, and facilitate a rapid response in the event of a complete system failure or natural disaster. After a preliminary market analysis, the project focus narrowed further to fill two particular roles within this first-warning surveillance mission: power line/pipeline surveying and forest monitoring.

The system and capabilities offered to a potential customer will consist of UAVs, ground stations and relay units, and the appropriate training to use the equipment. Potential customers include government interests such as the Department of Transportation or forest regulatory agencies, private owners and operators of oil and gas lines, power lines, and owners of assets the potential of damage from disasters such as forest fires. The primary concern addressed by the system design is patrolling right-of-way and monitoring for unauthorized third-party infringement. Production strategies are a combination of in-house design and manufacturing of

airframe and related components, and integration of commercially available propulsion and sensor systems. The Systems Requirement Report gives further details regarding the intended business plan.

1.2 Concept of Operations

A concept of the intended method of operation of the UAS presented addresses the power/pipeline and forest monitoring missions, respectively. Following is an abbreviated summary; the Systems Requirement Report gives further detail on the concept of operations.

Figure 1-1 shows a graphical summary of the pipeline mission. To examine a length of power/pipeline, the team defined the system in repeatable segments, determined by the full desired range of operation. Each segment consists of ground stations at both ends and an appropriate number of relay stations between to speed transmission of data from the UAV in flight back to the ground stations. The ground stations themselves consist of a mobile command and control center, a rough landing strip, and appropriate maintenance equipment. Station operations require only two individuals. The station acts as a node to collect incoming data and serves as a remote operating point should the aircraft need manual piloting. The UAV takes off from these stations and cruises to the start of the inspection point – a maximum of 10 miles distant. From here, the vehicle cruises at approximately 1000 ft AGL and 100 kts while performing inspections using a LIDAR sensor array and visual/thermal cameras. The end of the inspection run places the UAV within range of the second ground station, where it will land, refuel, and takeoff again back to the original station. Depending on the customer's requirements for inspection frequency, multiple aircraft may be in the air flying the route described above.

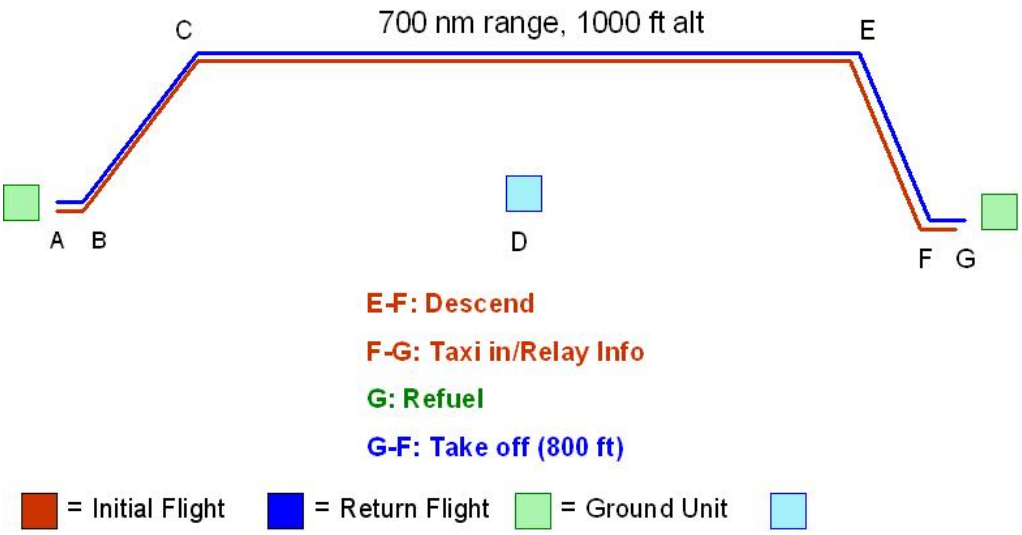

Figure 1-1. Pipeline mission synopsis

The forest mission is similar, but only utilizes one ground station at a maximum distance of 50 nm from the inspection area. Figure 1-2 shows an overview of this mission. UAVs take off from the station and proceed to the desired region, at which they perform their inspections in a wide "Z" pattern. The forest mission utilizes the same sensor package. Again, customer requirements for frequency of coverage dictate the number of vehicles in the air at any given time.

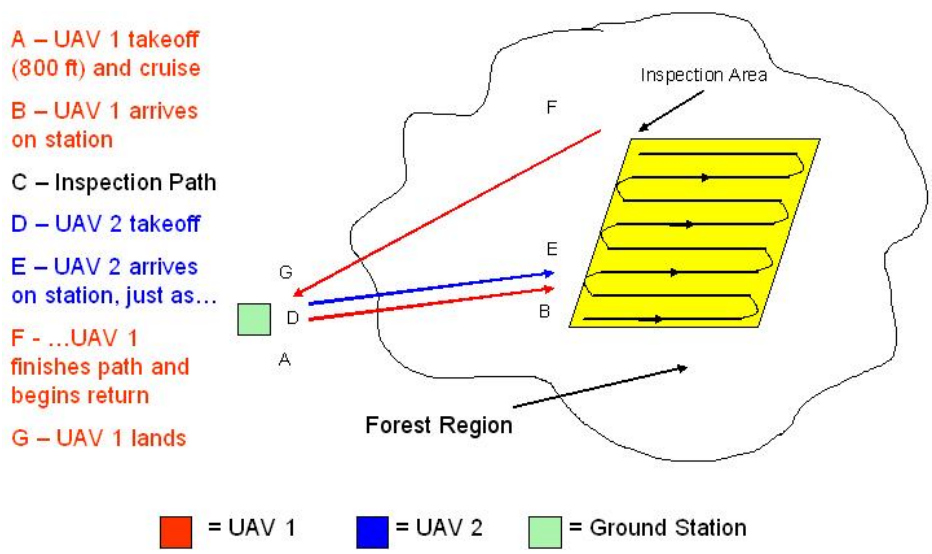

Figure 1-2. Forest mission synopsis

2 Major Design Requirements

The initial focus at the outset of this project emphasized the design requirements necessary to create an appealing product for the customer. Various paths of research, including design team generated ideas and direct contacts in the pipeline industry, yielded a set of customer requirements and accompanying engineering characteristics.

2.1 Customer Attributes

The customer requirements are organized and analyzed by way of a Quality Function Deployment (QFD) diagram, shown in Appendix A. Here the voice of the customer – the customer "what's" – interact directly with the necessary engineering characteristics – the engineering "how's". The requirements sought by the customer are broken down into three principle categories, shown below in Figure 2-1: performance, maintenance and cost, and mission operations. The performance of the system are those attributes that directly impact the capability of the aircraft and its components to effectively carry out its primary purpose – the monitoring and inspection of pipelines, power lines, and forest regions. Examples include efficiency, ability to provide continuous coverage, ability to operate autonomously, and robust operation in varying weather conditions. The mission operations segment includes such things as ease of operation (minimizing the necessary amount of labor), cost of operation, and environmental impacts. Desired maintenance and cost attributes include minimizing man-hours, reducing costs of maintaining the system, as well as designing a mobile and easily transportable vehicle.

WHAT	Performance	Efficient Speed
		Continuous Coverage
		Operate in Mountainous Terrain
		Ability to follow lines, circle at reasonable rate
		All Weather Operation
		Autonomous Operation
	Maintenance & Training	Ease of Maintenance
		Low Maintenance Cost
		Upgradeable
		Setup with Minimal Labor
		Fits in a Truck/Easily Transported
		Little Training Required to Operate
		Little Training Required to Repair
	Mission & Operations	Quickly Alerts to Trouble
		Easy to Operate Manually
		Integrated System
		Robust t/o Capability
		Able to See and Avoid Obstacles
		Low Environmental Impact (noise, pollution)
		Low Operational Cost

Figure 2-1. QFD customer requirements

2.2 Engineering Requirements

Customer attributes define the engineering characteristics of the UAV, each in response to one or more attributes. These "how's" are the driving factors of the design, providing quantifiable measures of the successful adherence to the customer's needs. The upper row of the QFD contains these engineering characteristics. Examples include number of operators (affecting cost and ease of operation), stall speed (affecting many of the performance attributes), endurance (shown as fuel capacity in hours), and power to weight ratio. Table 2-1 shows a

summary of these attributes. The numerical importance values accompanying them are values determined by the design team after pursuing a wide variety of research and discussion. The values indicate the level of "importance" a customer would place in a particular attribute.

Table 2-1. Engineering characteristics

Engineering Attributes	Importance (Absolute)	Improtance (Relative)
gps Accuracy (in)	243	10.90%
Number of Operators	225	10.09%
Sense and Avoid Accuracy (ft)	211	9.47%
Engine Efficiency	201	9.02%
Communication Relay Time (secs)	190	8.52%
Empty Weight (lbs)	162	7.27%
Number of Systems	162	7.27%
Operational Altitude (ft AGL)	134	6.01%
Endurance [hrs]	124	5.56%
Payload Capability (lbs)	123	5.52%
Time between Overhauls (hrs)	118	5.29%
Operational Speed (mph)	107	4.80%
Stall Speed (C_l max)	93	4.17%
T/O Length (ft)	87	3.90%
Designed Life (flight hrs)	49	2.20%

3 Payload

The information acquired by the payload is vital for the customer. It is imperative that the payload selected is efficient and will satisfy all of the customers needs in order to insure a successful product. The payload is also the driving factor behind the design of the aircraft; it puts restrictions on the sizing of the aircraft due to the requirements of housing and operating the payload from the air. Therefore, considerable thought and research goes into the overall selection of the payload. The following sections will provide an overview of the selected payload, the requirements of the payload, and the purpose of the payload components.

3.1 Objective of Payload

The payload defined for the continuous coverage UAV consists of an advanced sensor package. The objective of the payload is to provide surveillance and report detailed information about each mission type. The payload should have the ability to scan the ground around power lines, pipelines and the forest in detail and monitor necessary fields of interest. After speaking to a representative from the DOT and research concerning the observation interests of each industry, the mission required a combination of sensors to make a highly effective surveillance tool.

3.2 Component Selection and Sizing

In order to give the customers a product that would service their exact needs, several options needed research for sensor package that would be aboard the UAV. The research resulted in the determination that a combination of LIDAR (Laser Imaging Detection and Ranging) and an IR/Visual camera would provide the best surveillance options for the customer.

COTS products provide an effective sensor package, as well as keep costs low for the designed UAV. These products are the Litemapper 2400 LIDAR system by IGI (Ingenieur-Gesellschaft fur Interface mbH) [4] and the Mini POP IR/Visual camera by IAI (Israel Aerospace Industries Ltd.) [5].

The Litemapper 2400 is a LIDAR system designed for low flying ultra light aircraft and is best suited for pipeline and power line monitoring. Its main advantages are small size, low weight and a high geometrical accuracy [4]. This system includes a Computer Controlled

Navigation System (CCNS), which provides continuous guidance, attitude and positioning data to the LIDAR. The CCNS is a necessary part of the payload package. The Litemapper 2400 weighs 13 lbs and has dimensions 1.8 x .66 x .71 ft. The CCNS weighs 9 lbs and has dimensions .82 x .69x .43 ft for a total LIDAR package weight of 22 lbs and a volume of 1.1 cubic feet.

The Mini POP (Plug-in Optronic Payload) IR/Visual camera, designed to be a small UAV observation platform, provides thermal imaging as well as day/night observation capabilities. The camera weighs 20 lbs and has dimensions .66 (d) x 1.1 (h) ft. Table 3-1 gives a summary of the payload weights and dimensions. In addition to the weights tabulated in this table, an additional 40% of the computed payload weight adds to the payload to account for installation and operation weight making the total payload weight approximately 60 lbs.

Table 3-1. Sensors Specifications.

			Power Consumption	
	Weight (lbs)	Dimensions (ft)	W	hp
LIDAR	13	1.8x.66x.71	30	0.04
CCNS	9	.82x.69x.43	25	0.034
IR / Visual Camera	20	.66(d)x1.1(h)	100	0.134
Total	42	1.5 ft^3	155	0.21
Installation Weight (40% of Total Payload Weight)	17	N/A	N/A	N/A
Power From Alternator	N/A	N/A	1500	2

The payload package itself does not require excessive amounts of power to operate. The LIDAR and the CCNS together only require 55 W of power to operate (.074 hp). The IR/Visual camera requires the most power at 100 W (.134 hp) and the total payload power requirement should be approximately 155 W or .21 hp. With this small amount of power consumption, it is estimated that the energy can be bled off the engine using its built in alternator. The alternator itself has a maximum power output of 1500 W (two hp). This amount of power is more than sufficient to run all the necessary payload components as well as any subsystems that may also need to power to operate, such as servo motors for control surfaces. Table 3-1 gives a summary of the power requirements for each system.

3.3 Payload Operations

The driving sensor aboard the UAV is the IR/Visual camera. This sensor package is

imperative in the inspection mission of all three mission types. These sensors serve two functions. First, they provide continuous thermal imaging. As a result, inspectors can track if a pipeline/power line is maintaining ideal temperatures. For example, if a power line is about to experience electric shortening, inspectors can detect the rise in the power line temperature and prevent the potential problem. Similarly, during a forest fire, the heat caused by the fire can provide rescue workers with exact conditions of the forest. The camera will also allow them to distinguish between hot and smoldering fires. Second, the video tracking features of the camera are used to observe the surface conditions surrounding the pipeline and power line. This allows inspectors to monitor for any unauthorized activity or encroachment taking place near their product. According to the voice of the customer, intruders damaging and stealing from pipelines is one of their main concerns, and the inclusion of an IR/Visual camera to the sensor package provides the DOT with the resource to monitor intruders. In addition to observation specific tasks, these cameras allow manual operation of the UAV by an operator. The UAV design allows the IR/Visual camera to run continuously throughout the mission. This is to allow an operator the ability to fly the aircraft remotely during any segment of the mission. In the event of a malfunction or sudden change to the mission profile, the operator can then take the immediate action needed to return the UAV to safety. In addition to manual flight, the camera can also add the capability of see and avoid technology. By having the camera in operation continually, the aircraft can use this information to identify hazardous objects, such as other aircraft or structures, and offer alerts or perform the necessary maneuvers to avoid such objects.

LIDAR is the other sensor onboard that provides the user with useful data concerning topographical assessment. LIDAR has the ability to measure and scan ground topography at a rate of 20,000 coordinates per second. This feature is vital for pipeline and power line inspection. Inspectors within these two industries can use the UAV to detect any geological changes, such as land shifts, erosion or vegetation encroachment. In the event that any serious changes occur to the pipe or power lines, inspectors can prevent damages that these geological changes might have upon the structures. Furthermore, LIDAR conducts land surveying so that building and installations of future pipeline and power lines can be determined. In other words, inspectors will know if a land is structurally stable or not and if it can be used for pipeline/power line installation. In addition to these benefits, LIDAR is extremely useful for the forest industry. It can accurately scan and determine the vegetation density of a forest as well as determine

vegetation types. Inspectors in the forest industry can use this information to monitor general forest health, as well as monitor and analyze forest fires [4].

The designed UAV will also include a LIDAR Controller, or a Computer Controlled Navigation System (CCNS). The CCNS provides continuous guidance, attitude and positioning data to the LIDAR. LIDAR works optimally if the UAV stays dynamically stable at all times and if the altitude is 650-1300ft above ground level (AGL). However, if the UAV starts to oscillate and move, or if the altitude reaches above 1300ft AGL, the data that the CCNS provides will allow LIDAR to adjust its settings and scan the ground accordingly. In other words, LIDAR does not lose significant accuracy when it is not facing ideal conditions. LIDAR can scan the ground at any altitude but achieves the best resolutions at a range of 650-1300ft AGL. For the proposed mission profile, it is determined that the UAV will scan the ground at an altitude of 1000ft AGL, which falls within the optimal range of operation for the LIDAR sensor. LIDAR and its controllers are insensitive to temperature variations and acceleration changes. This means that if a UAV was to survey a pipeline in the Middle East, where it is extremely warm, or a power line in Alaska, where the temperatures are frigid, the same LIDAR package accomplishes the task. In addition, since the CCNS is a multi-functional system, controller tasks for the LIDAR unit from the ground are minimized [4]. It is not necessary for the LIDAR to run continuously throughout the entire mission. Operators will have the option to choose when and where to operate the LIDAR system. More than likely, operators will choose to have LIDAR in operation only during cruise or sections of the cruise portion of the UAVs' designed mission. As an added benefit, by having LIDAR in operation only when necessary the aircraft runs more efficiently. There is less of a power draw on the engine therefore resulting in better fuel efficiency for the aircraft engine. This leads to an overall reduction in operation costs beneficial to our customers.

4 Aircraft Sizing Method

Sizing an aircraft is a difficult process that involves many variables with no single solution. Many aircraft configurations have the potential to work, but not all of them are optimal for the designed mission. Likewise, for any given mission, there are multiple segments to optimize the aircraft for, but discerning the best segment is requires analysis and an understanding of the underlying needs of the customer. For example, in some military aircraft, it may be necessary to sacrifice some weight to provide protection for the pilot, therefore making costs less of a driving factor. In the case of Oculus Superne, keeping cost minimal while still providing ideal conditions for sensor package operation are of the utmost importance. The section below describes how the UAV was optimized using both commercial software and carpet plots; it also gives some details of the sizing code results.

4.1 Sizing Code

ACS version 4.1.10 by Avid is the sizing code used. The code offers several types of equations based off empirical curves that allow for the various differences between large commercial, military and general aviation aircraft. Though the code offers various data sets for different classes of aircraft, there is not yet a set of empirical equations for UAVs available through ACS. Based off the information known about the final size of the UAV, the team used general aviation weight equations to model the. The tail volume coefficient method, as outlined in Raymer's text, helped in determining tail sizing accurately because the tail configuration chosen during the Pugh's method was different from the types available in the sizing code. This method is also specified in ACS; the results of which are compared to hand calculations, as discussed in Section 7.

Early in the design process, an estimate of the needed engine power was completed, and an off the shelf unit was selected. Using this fixed engine approach, the maximum power, the weight, and revolutions per minute become fixed inputs to the sizing codes. No batteries or auxiliary power units are necessary for this particular engine. The sizing code also uses propeller specifics such as propeller efficiency and diameter as inputs. Table 4-1 shows these fixed ACS inputs.

Table 4-1. Fixed ACS inputs.

Power [hp]	40
Installed Weight [lbs]	48
RPM	4500
Propeller Efficiency	0.821
Propeller Diameter [ft]	2.5

Table 4-2 gives several other sizing code inputs. C_{Lmax} is a reasonable estimation of the UAV's lift coefficient. An assumed average operational altitude of 5000 ft MSL accounts for various mountainous terrains the UAV will encounter. This includes the 1000 ft AGL operation condition as specified in the mission profiles. This also optimizes usage of the sensor package. The velocity shown in Table 4-2 originated from offering a reasonable rate of coverage, which was determined to satisfy the customers' requirements of frequent coverage. The range is a result of the mission profile for the pipeline, assuming 1300 nautical miles to be the average pipeline length. Finally, the payload weight is the weight of the installed package including LIDAR, CCNS and the IR/visual camera. The mission segments used were takeoff, acceleration, climb, cruise and landing.

Table 4-2. Sizing code variable inputs.

C_{Lmax}	1.5
Cruise altitude [ft MSL]	5000
Velocity [kts]	100
Range [n.m.]	1300
Payload Weight [lbs]	60

4.2 Carpet plots

Carpet plots optimize a design by finding the lowest weight design point using relative constraints. Several possible constraints include landing distance, takeoff distance, ceiling height and stall speed. In this case, an investigation of the ceiling and stall speed illustrate that they did not influence the UAV design. The constraints that have decided the design point of the UAV are a landing constraint of 550 ft and a takeoff constraint of 925 ft. Both lengths include ground

roll and clearance of a 50ft obstacle. Figure 4-1 represents these as the dashed light-green line and the solid black line respectively. With no engine selected, a typical carpet plot varies wing loading and power to weight ratios. With the engine for this UAV fixed, power to weight as a variable is not useful; instead, aspect ratio is used in Figure 4-1.

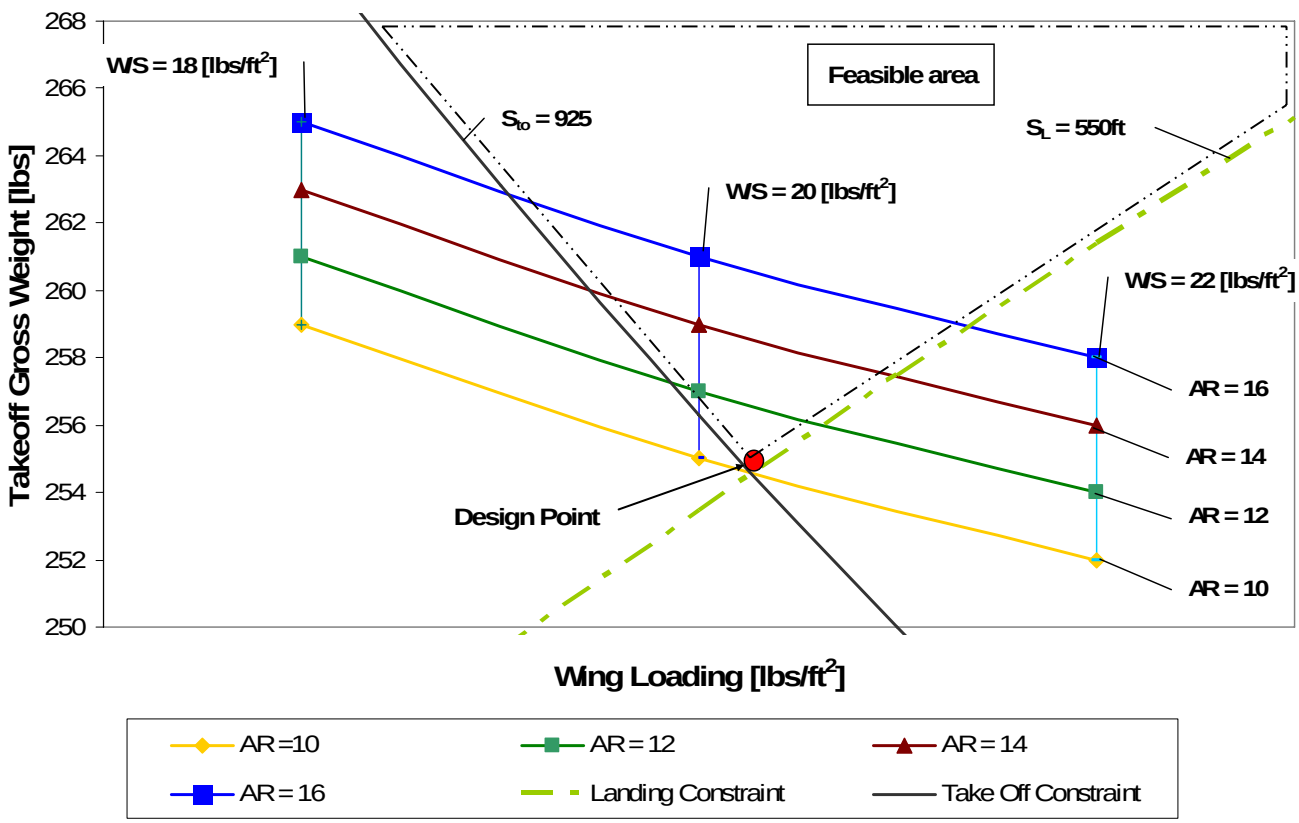

Figure 4-1. UAV carpet plot.

Varying values of aspect ratios, such as 10, 12, 14 and 16, along with wing loading values of 18, 20 and 22 pounds per square foot form a matrix to produce Figure 4-1. The gross takeoff weight was found for each point in the matrix by using the output from ACS. The plot of gross weight versus wing loading created nearly linear lines for each value of aspect ratio. The black dashed line encloses the area of feasible designs, the area where designs meet the minimum constraints. The red dot in Figure 4-1 displays the design point for the UAV. It corresponds to an aspect ratio of 10 and a wing loading of 20.3 lbs/ft^2. Table 4-3 represents the

output after placing these values back into ACS. The output of the sizing code suggest that the UAV will have an estimated endurance of 14.38 hours, a wing area of 12.55 feet squared and an lift to drag ratio of 13 during cruise. Appendix C contains a copy of the entire ACS output.

Table 4-3. Output from ACS.

Gross Weight [lbs]	255
W/S [lbs/ft^2]	20.3
Aspect Ratio	10
Wing Area [ft^2]	12.55
Endurance [hrs]	14.388
Take off Distance [ft]	915.6
Landing Distance [ft]	537.7
Fuel Weight [lbs]	39
L/D	13
Power/Weight [hp/lbs]	0.15
Cruise SFC [lbs/bhp/hr]	0.487

4.3 Code Validation

The sizing code uses empirical data to create curves for vehicles in the class of equations chosen. The above case uses general aviation component weight equations. The designed UAV is much smaller than general aviation aircraft and in many cases the code must interpolate data. To ensure that ACS output is reasonable, the team performed two validation checks, one using a constraint diagram, the other using empirical data from a database of other UAVs.

Using equations relating power to weight and wing loading, a constraint diagram graphically displays the constraints on an aircraft. The values in Table 4-4 generates Figure 4-2 with the same takeoff and landing constraints as used in the carpet plot and the addition of a 2g maneuver constraint and a straight line flight constraint. The constraint diagram acts as a check to ensure that the design does not exist outside of the constraints on the carpet plot. In Figure 4-2, the red line representing the 2g maneuver constraint, the blue line representing the strait line flight constraint and the green line representing the landing distance constraint borders the envelope of feasibility. The red dot is the design point given by the carpet plot; it is at a power to

weight ratio of 0.15 horsepower per pound and a wing loading of 20.3 pounds per square foot. The design point rests within the envelope.

Table 4-4. Constraint diagram inputs.

Aspect Ratio	10
C_{Lmax} (cruise) [kts]	1.5
C_{Do}	0.018
Cruise Velocity [kts]	100
2g Manuever Velocity	85
Climb Rate [ft/s]	10
Oswald Efficiency Factor	0.8
Propeller Efficiency	0.821

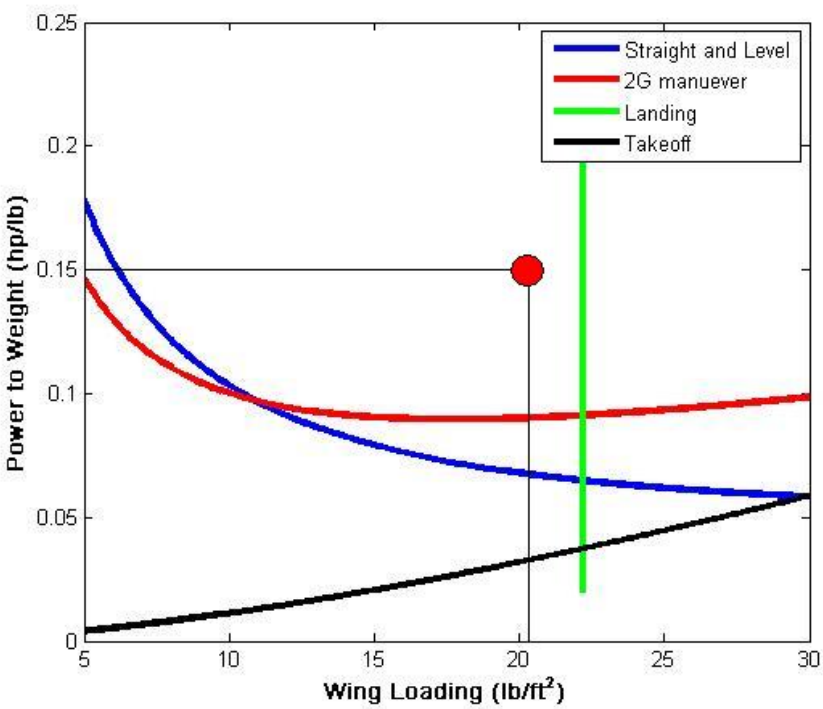

Figure 4-2. Constraint Diagram.

Early in the design process, Oculus Superne created a database of aircraft of varying types of fixed wing UAVs. This database includes, among other things, empty weights, payload weights, gross takeoff weights, endurances, and velocities for a large number of vehicles. This

database, helped to generate Figure 4-3 that shows the gross takeoff weight as a function of the payload weight. There is a small amount of scatter, but the R^2 value of over 90% suggests that it is a reasonable fit. The equation of the trend line created from over 50 points yields an expected gross weight of 207 pounds for a UAV with a 42 pound payload. Figure 4-3, however, does not take into account the endurance of the aircraft giving a plausible explanation of the 20% marginal difference in the ACS and empirical gross takeoff weight.

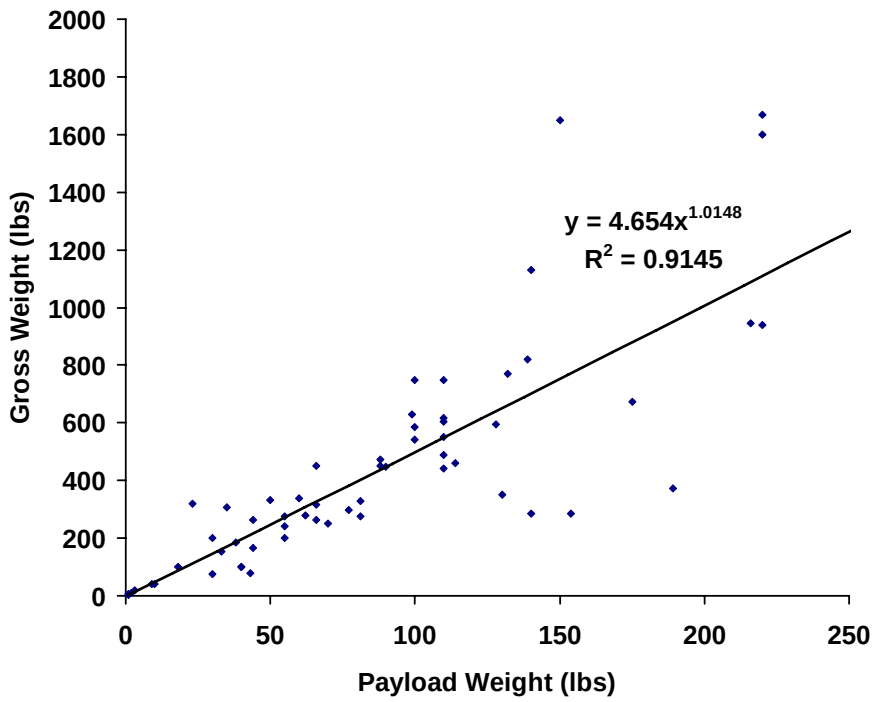

Figure 4-3. Gross weight as a function of payload weight from UAV database.

Figure 4-4 is another plot from the database of UAVs, but this plot shows gross takeoff weight as a function of endurance. The equation of the trend line presented in the figure with an endurance of 14.388 hours produces a weight estimate of 430.9 pounds. There is a significantly high amount of scatter in Figure 4-4, less than 37%. This may account for the 68% difference between the ACS and empirical weight estimates. The ACS weight estimate lies between the empirical weight estimates associated with Figure 4-3 and Figure 4-4, and considering the amount of scatter in each, the sizing code approximation seems feasible.

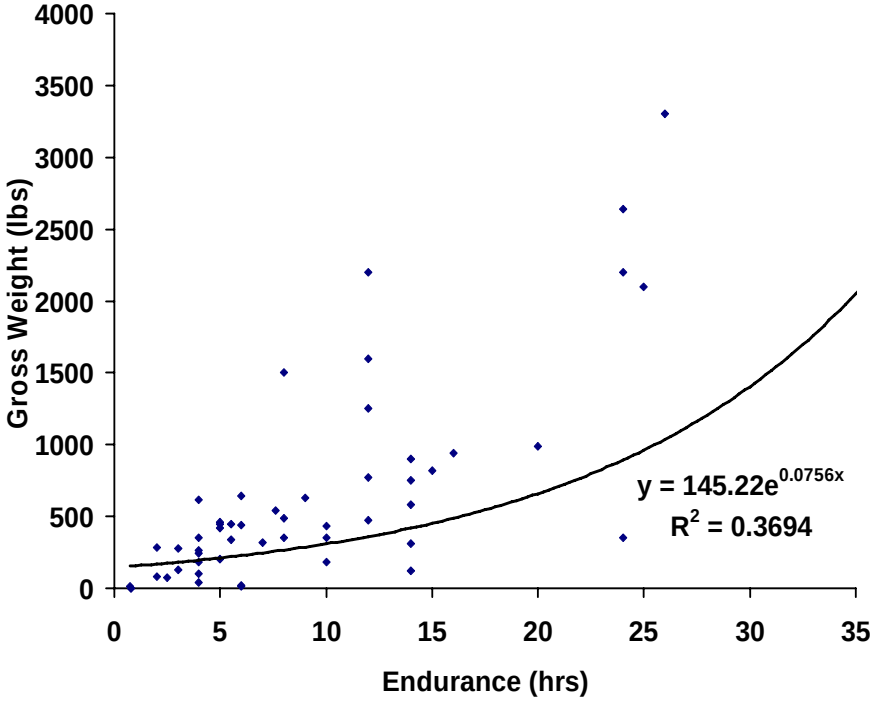

Figure 4-4. Gross weight as a function of endurance from UAV database.

5 UAV Design

The final UAV design for the frequent area coverage mission is a pod fuselage, pusher propeller, high aspect ratio and inverted V tail vehicle. It provides all the mission requirements, while housing the payload in such a way that it will minimize volume and optimize performance. The design also satisfies most of the threshold values, which represent the target characteristics the team designed to.

The payload and engine define the body size because these are what must fit into the fuselage in certain locations. ACS defined the wing sizing, while the boom length is a function of stability and weight. Table 5-1 shows some of the important aircraft sizes.

Table 5-1. Sizes of the current aircraft components.

Wing Span	11 ft
Chord Length	1.15 ft
Wing Area	12.6 ft^2
Propeller Diameter	2.5 ft
Fuselage Height (Front)	1.08 ft
Fuselage Height (Back)	.92 ft
Fuselage Width (Front)	2 ft
Fuselage Width (Back)	1.5 ft
Fuselage Length	5.5 ft
Boom Length	4.33 ft
Boom Seperation	3.17 ft

5.1 External Design Features

To comprehend the final UAV design it is essential to see a scaled model of the aircraft. This model demonstrates all of the important features of the aircraft. In addition, the model could undergo further structural and aerodynamic evaluation in the future if necessary. Figure 5-1 shows the current model, which represents the UAV for all the known information.

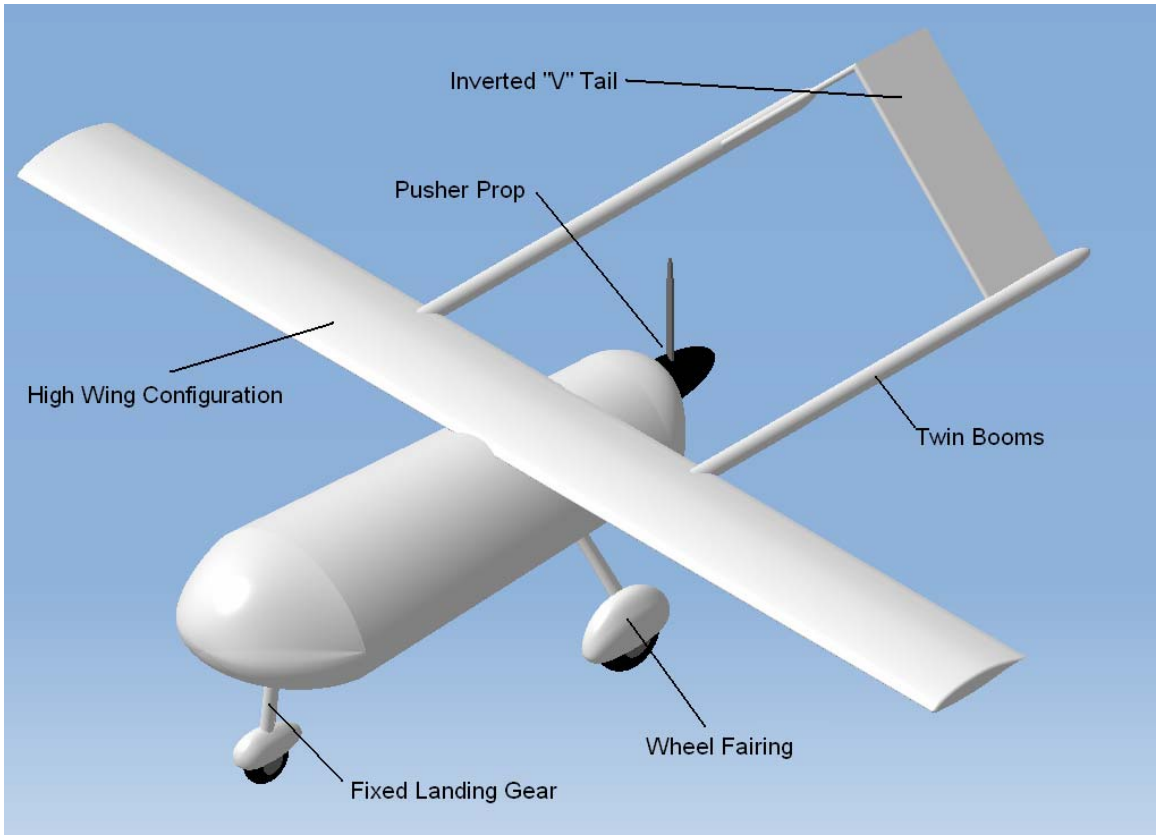

Figure 5-1. External Walk-Around Chart

The walk around of the chart shows some of the key features of the UAV design. As mentioned earlier, the fuselage of the aircraft is a pod shape to maximize the internal volume. Unlike a typical cylindrical shaped fuselage, this feature minimizes excess fuselage, reducing surface area and therefore reducing drag. If designed correctly the fuselage could even produce some lift.

With the engine mounted in the back of the aircraft, a pusher propeller configuration is the result. Twin booms feed off the wings, spaced symmetrically from the vertical center of the aircraft. They support the inverted "V" tail configuration, which is in place of the standard tail arrangement due to the use of the pusher propeller design.

Figure 5-1 also shows that the UAV has a high wing configuration. Initially the aircraft had a low wing configuration to provide structural support for the landing gear. However, after reviewing the landing gear design and aerodynamic performance of each wing position, a high wing system proved paramount. A high wing arrangement provides a higher L/D than a low wing arrangement and a low wing configuration is not critical to provide structural stability to

the landing gear. Historical data from previous UAVs of a similar configuration also show a high wing design is more desirable.

The landing gear itself is a fixed system that will reduce the complexity and cost of the aircraft. It however, will produce more drag than retractable landing gear. Wheel fairings placed over the tires of the landing gear aid in reducing some of the extra drag. This does not fix the problem, but significantly aids in reducing the drag from the wheels. The struts themselves are a symmetric airfoil shape. This design feature minimizes the amount of parasite drag from the fixed landing gear system.

5.2 Important Internal Design Features

The key to a successful early design is to understand the basic internal layout of the aircraft. The internal walk-around layout provides a clear and concise visual representation of how the internal components fit within the aircraft. For the current aircraft concept, the internal components consist of all the payload hardware, avionics, engine, fuel tanks, fuselage fuel and the wing box.

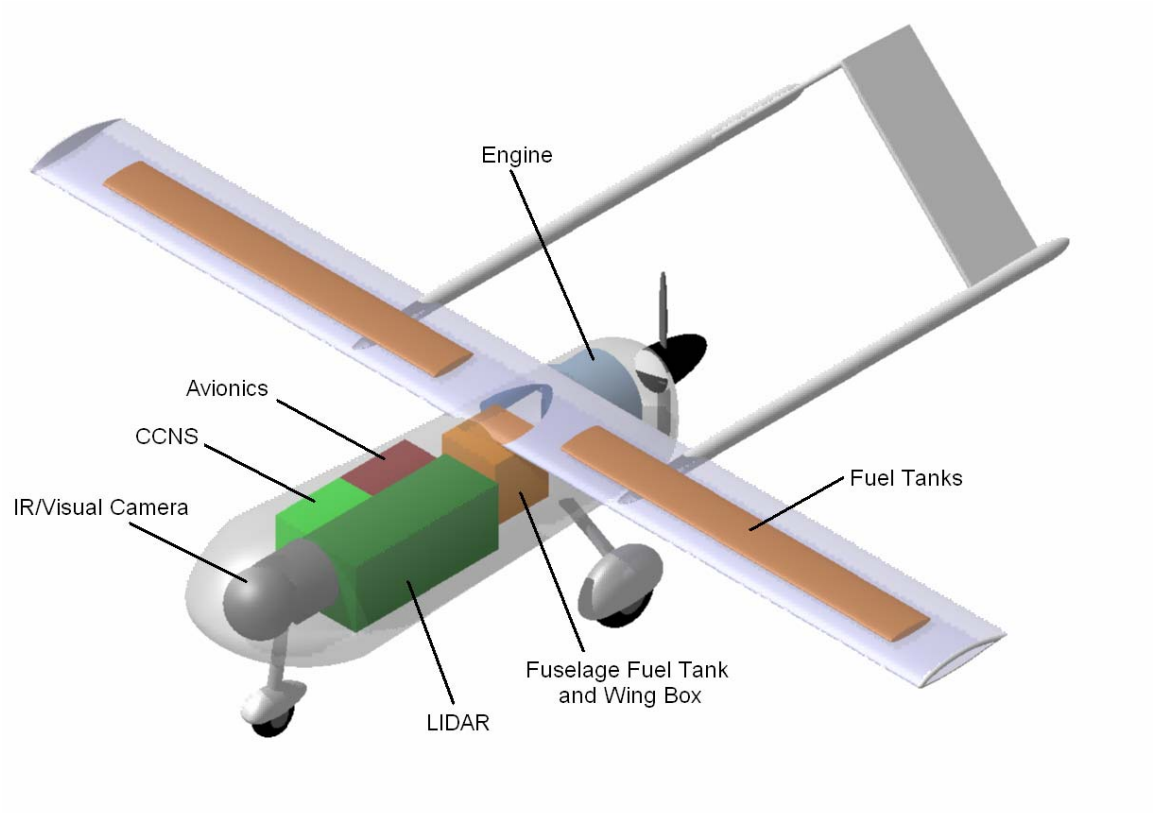

Figure 5-2. View of Internal Layout

Figure 5-2 shows the three dimensional view of the internal layout of the UAV. It is obvious that all the components take full advantage of the internal space avoiding extra empty volume in the fuselage. As stated previously, this is a key design feature to the UAV.

Since the most important aspect to the vehicle is the capability to visually analyze a specified area, it is essential that the camera is located at the nose of the aircraft. This location allows the camera to focus anywhere from vertical to horizontal relative to the ground without internal or external hardware obstructing the camera view. One of the main reasons the engine is in the rear of the aircraft is because the camera is in the nose. If the engine were to be a puller propeller, it would obstruct the view of the camera and would cause unwanted vibrations from the engine. This, among other reasons already outlined, is why the engine is located in the rear of the aircraft.

The LIDAR sensor is located in the middle right section of the fuselage. It is oriented in a way such that it will be able to sense information directly below. The placement for the LIDAR will allow it to function optimally without any interference from engine vibrations or obstructions. The CCNS and avionic hardware are located directly left of the LIDAR. This keeps all the control systems forward of the wing box, keeping the center of gravity in front of the aerodynamic center producing a stable aircraft. In addition, minimum wiring results by having the CCNS and avionics next to the LIDAR and camera. This keeps installation weight and complexity down. Installation weight may seem minute, but every extra pound of weight reduced from the aircraft directly reduces operating costs.

The wings of the aircraft house the main fuel tanks. Figure 5-2 shows that the fuel tanks extend inside a portion of the wing. Keeping the fuel tanks in the wing saves a substantial amount of room in the fuselage. However, if a potential problem arises with the wing fuel tanks, the fuselage design incorporates extra room for fuel. A potential problem may include spar and rib location in the wing, which could potentially decrease the size of fuel tanks. The position of the fuel relative to the engine is also a key design feature. Having the fuel close to the engine will limit the amount of extra piping needed to transfer the fuel. This may also have an affect on the size of the fuel pump needed.

5.3 Views of Aircraft to Scale

The top and back view of the aircraft shows many important aspects of the UAV design. Foremost, it shows that aircraft is eight foot nine inches long overall from nose to the back of the inverted "V" tail. The wing has a span of 11 feet with a chord of one foot two inches. The fuselage has an overall length of five and a half feet but can be broken down into components. The nose is one foot long and the rear engine cover is six inches long. The rest of the fuselage accounts for four feet of the total length. The booms are separate from each other by three feet two inches. This allows the two and a half foot propeller to have four inches of clearance between it and the booms on each side. In addition, the chord of the inverted "V" tail is around 10 inches. Figure 5-4 shows the tail itself has a 90º angle in the "V" of the tail. This figure also illustrates that the main landing gear tires sit 11.6 inches from the center of the nose landing gear.

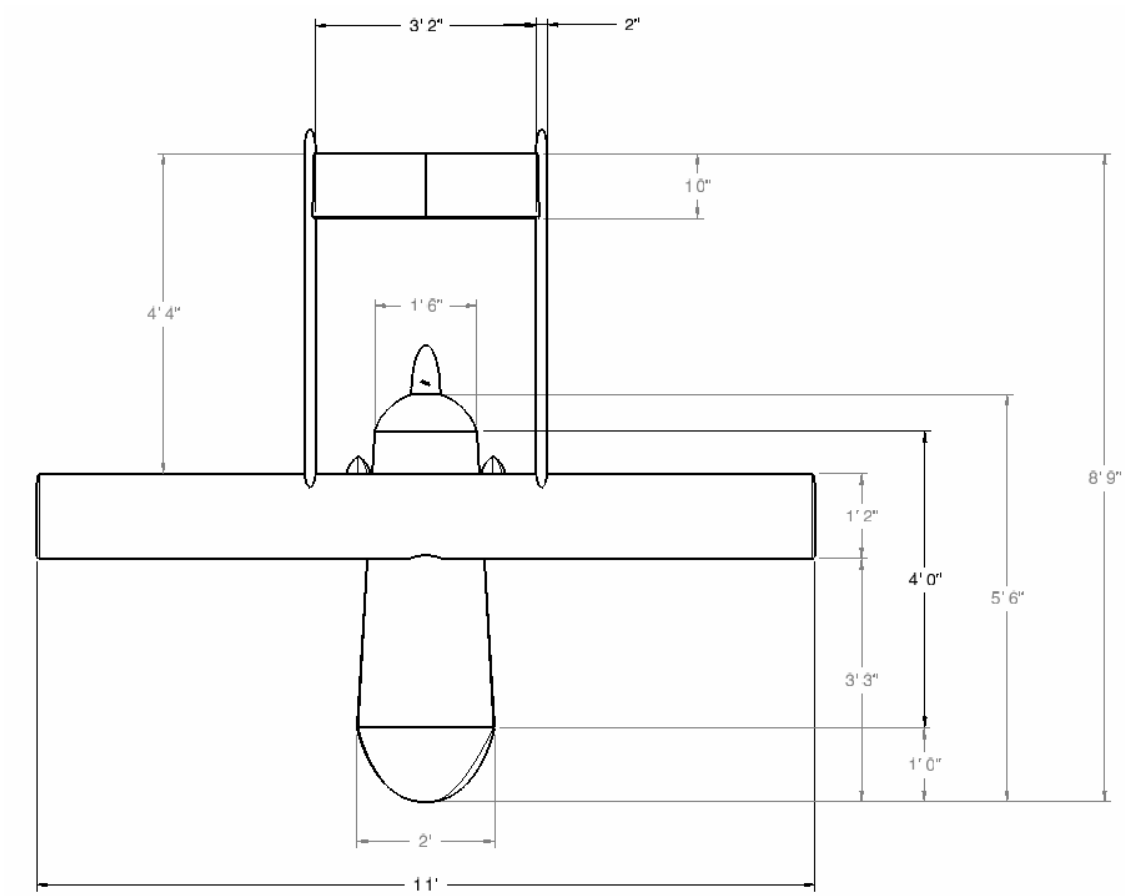

Figure 5-3. Top view of the UAV

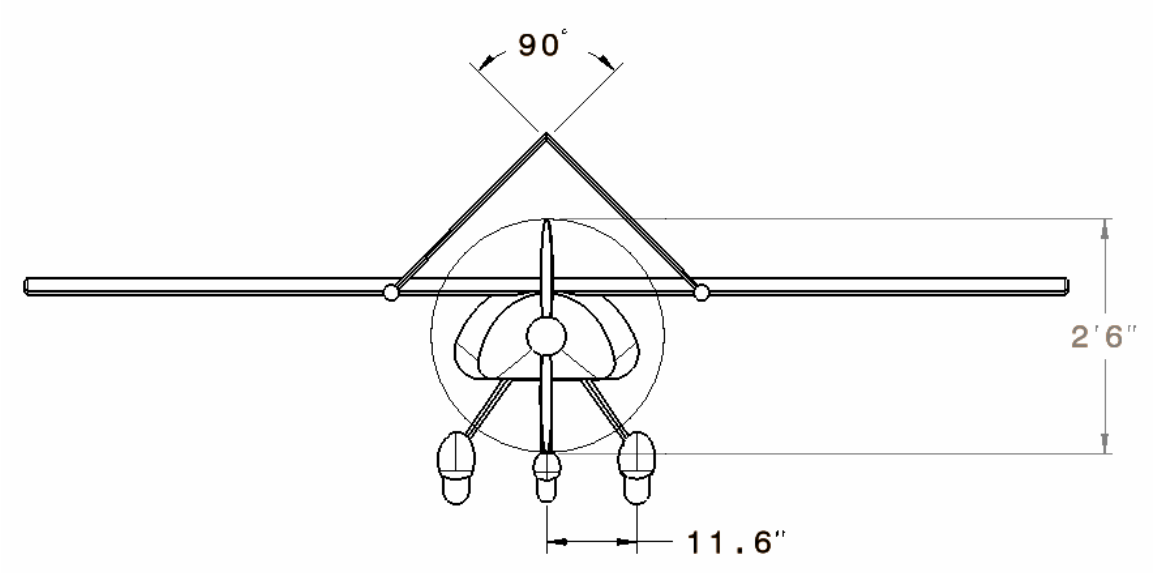

Figure 5-4. Back view of the UAV

Figure 5-5 shows the side view of the aircraft and some of the important dimensions. A key feature of this figure is the height of the front and back of the fuselage. The front of the fuselage is one foot one inch and the back is 11 inches. This shows that the fuselage gradually gets smaller as it moves aft. In the next section, a computational method shows how the landing gear dimensions transpire. Figure 5-6 shows the front view of the aircraft.

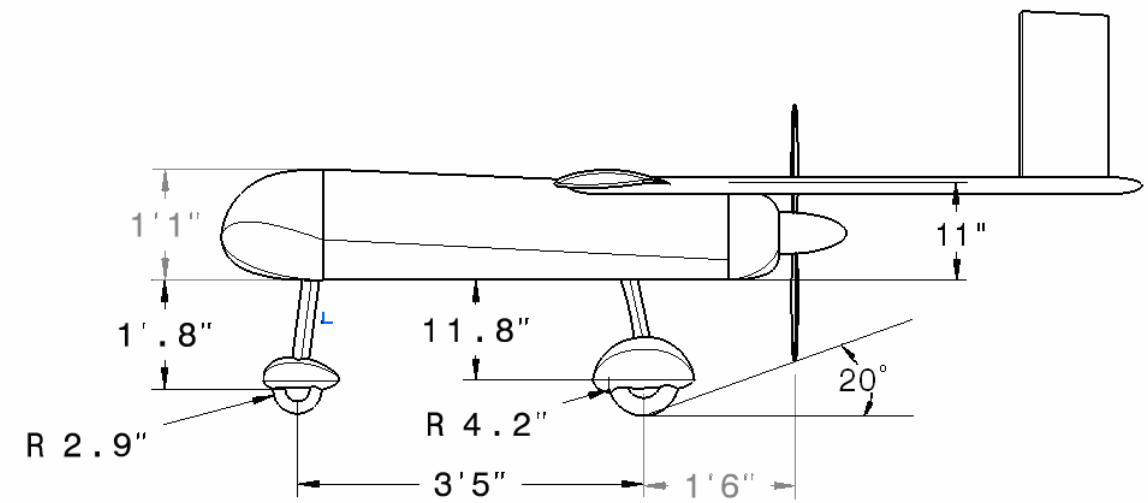

Figure 5-5. Side view of the UAV

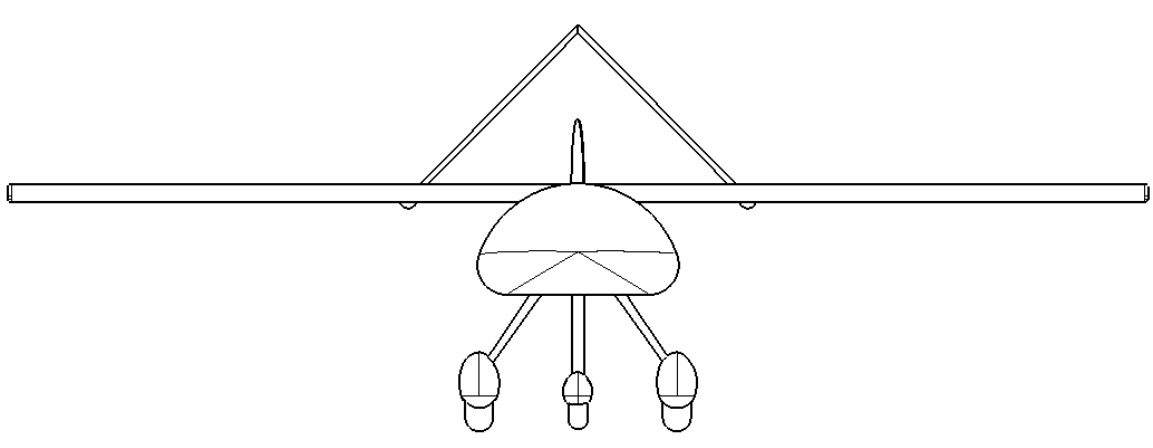

Figure 5-6. Front View of the UAV

Figure 5-7 shows the internal components of the aircraft dimensioned from the nose to the center of each component. As seen in the figure the camera sits eight inches back from the front of the nose. The LIDAR falls two feet one inch from the nose while the CCNS and avionics sit next to it. The fuel tanks in the wing are placed three feet eight inches from the nose. The size of the tanks is four feet two inches long with an ellipse profile being six inches in diameter and one inch along the semiminor axis. The fuselage tank and wing box area is located under the front of the wing at three and a half feet from the nose. The engine sits further back near the propeller so the shaft going from it to the propeller is not long.

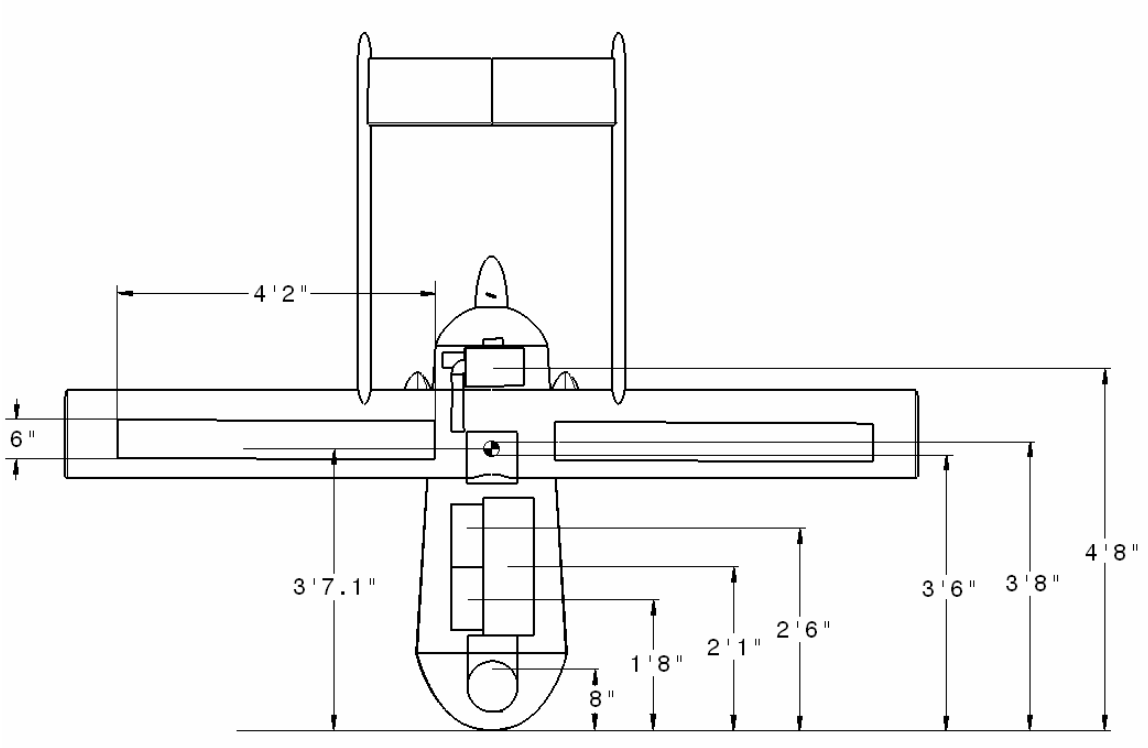

Figure 5-7. Internal Dimensions of the UAV

5.4 Landing Gear Design

The landing gear was formulated using the equations expressed in Raymer's textbook. This book underlines some of the important features of the landing gear as well as some initial sizing estimates. For this aircraft, a tricycle landing gear layout is applied. This is a common configuration for aircraft of similar size and missions and is the most feasible arrangement for this design. Figure 5-8 below gives some basic parameter dimensions. B is the horizontal distance from the center of the nose landing gear wheel to the center of the main landing gear wheel. H is the height from the static ground level to the center of gravity. N is the horizontal distance from the center of the nose wheel to the center of gravity for both the forward and aft positions. M is the horizontal distance from the center of the main wheel to the center of gravity in both the forward and aft positions.

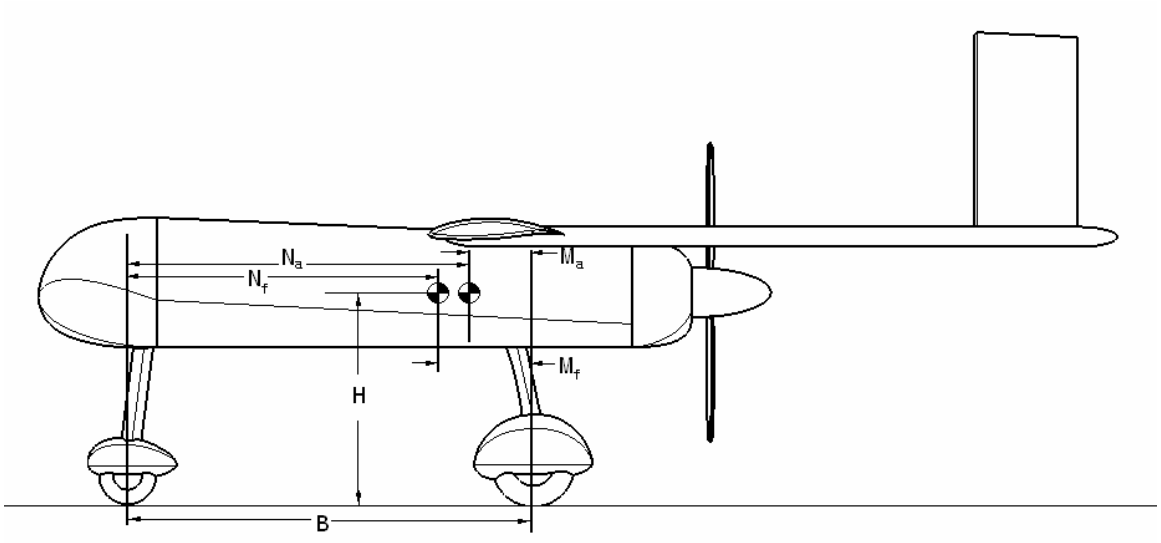

Figure 5-8. Landing Gear Geometry

The main concept behind the layout of the landing gear is to keep the center of gravity forward of the rear landing gear. This creates a stable aircraft at landing. Figure 5-8 shows that this method takes into account travel of the center of gravity.

The nose landing gear is 0.75 feet aft of the nose so that it will not impede the camera's view. Additionally, the main landing gear positioning allows for a 20° maximum tip back angle between the landing gear and the propeller. The tip back angle is the angle between the main landing gear wheels and the propeller or booms, depending on the length of the booms, in which, if the aircraft tipped back it would hit the ground. The design takes into account any irregularities that may occur from extra landing gear bending during landing, terrain fluctuations or tire pressure. Three facts helped systematically compute the unknown variables in Figure 5-8; the nose landing gear is set at a certain distance, the aircraft has a 20° tip back angle and the center of gravity resides at specific known positions.

The overturn angle is the angle between a main wheel and the center of gravity when looking at a main wheel from the back of the aircraft having a main wheel and the nose wheel aligned in view. The overturn angle provides the distance the main wheels should be from the center of gravity so that the aircraft does not tip over during sharp taxing turns. Common overturn angles range from 55° to 65°. Using a estimated distance between the center of the aircraft and the main landing gear and knowing the height of the center of gravity, a 61° overturn angle resulted, which fits in the range of acceptable overturn values. Figure 5-4 shows that the

final iteration of this procedure, which resulted in a distance of 11.5” from the center of the aircraft to the main landing gear. Later optimization for this distance may occur for structural or aerodynamic reasons. Table 5-2 shows the values of the landing gear variables.

Table 5-2. Landing Gear Variables

Variable	Value	Unit
B	3.465	ft
H	1.718	ft
M_a	0.615	ft
M_f	0.625	ft
N_a	2.850	ft
N_f	2.840	ft
Tipback Angle	20	degree
Overturn Angle	61	degree

The nose gear carries up to 10% of the max static load, while the main gear holds 90% of the total weight of the aircraft. The total weight used is a conservative design parameter of 300 lbs to account for any extra weight not predicted in the sizing code. The statistical tire sizing equations for general aviation aircraft outlined in Raymer’s textbook, give the tire dimensions for the aircraft using this value. All the equations needed to compute the tire sizing are below. D is the diameter of the wheel and W_i is width of the wheel. W is the total weight of the aircraft and W_w is the weight on the wheel being determined. For the main tires, this is 45% of the total weight and for the nose tire, this is the max static load on the nose.

Equation 5-1. Wheel diameter.

$$D = 1.51 W_w^{0.349}$$

Equation 5-2. Wheel width.

$$W_i = 0.715 W_w^{0.312}$$

Equation 5-3. Maximum Static Wheel Load.

$$(MaxStaticLoad)_{nose} = W \frac{M_f}{B}$$

The diameter of each wheel itself is 50% tire, while the other 50% is the hub. In addition, the tires need to be all-terrain capable so that the aircraft can takeoff and land from a rough field. Recommendations, from Raymer’s book, for maximum pressure in the tires are 45-60 psi for dry grass on hard soil, 30-45 on wet grass on soft soil, and 40-60 psi on hard packed sand. Using this information, a maximum pressure of 45 psi allows the UAV to perform its missions. With

this pressure comes a certain amount of compression in the tire. This compression on the wheels yield two main variables called the rolling radius (R_r) and the footprint area (A_p). The rolling radius is the radius of the tire between the ground and the center of the wheel after compression. The footprint area is the area of the tire that is in contact with the ground. Equation 5-4 and Equation 5-5 are the equations used to determine these parameters. Table 5-3 gives these values along with the tire dimensions.

Equation 5-4

$$W_w = PA_P$$

Equation 5-5

$$A_P = 2.3\sqrt{W_i D}\left(\frac{D}{2} - R_r\right)$$

Table 5-3. Dimensions of the Tire

Variable	Value	Unit
D_{nose}	5.843	in
W_{nose}	2.397	in
$R_{r\ nose}$	2.797	in
A_{pnose}	1.073	in^2
D_{main}	8.365	in
W_{main}	3.304	in
$R_{r\ main}$	3.631	in
A_{pmain}	6.667	in^2
Tire Pressure	45	psi

5.5 Propulsion System

The engine of the UAV will be purchased off the shelf from UAV Engines Ltd, model AR741. The most important characteristics considered include the maximum power, the installed weight, the maximum specific fuel consumption, and the revolutions per minute. A maximum power of 40hp fulfills all of the mission parameters. The AR741, a rotary engine, provides the necessary horsepower while offering a low installed weight. The maximum SFC is also high for this engine class. Table 5-4 gives important engine parameters including the type of fuel used, which is gasoline; an easily obtained fuel. The fully installed weight listed in the

table includes a generator to run the avionics, the sensor package and the control surfaces. The AR741 is capable of providing 1500 watts of constant power. The engine also provides all of the necessary power at the altitudes seen during operation as illustrated in Figure 5-9. It shows the required power as the red line that lies below the blue line that represents the available power. This is plot was done for altitudes below 15,000ft above sea level, which should encompass most operating conditions the UAV will see.

Table 5-4. AR741 engine parameters.

Max Power [hp]	40
Max RPM	7000
Engine weight [lbs]	23.5
Installed Weight w/ Generator [lbs]	48.2
Generator Capacity [V]	28
Generator Output [W]	1500
Fuel Type	Auto Gasoline

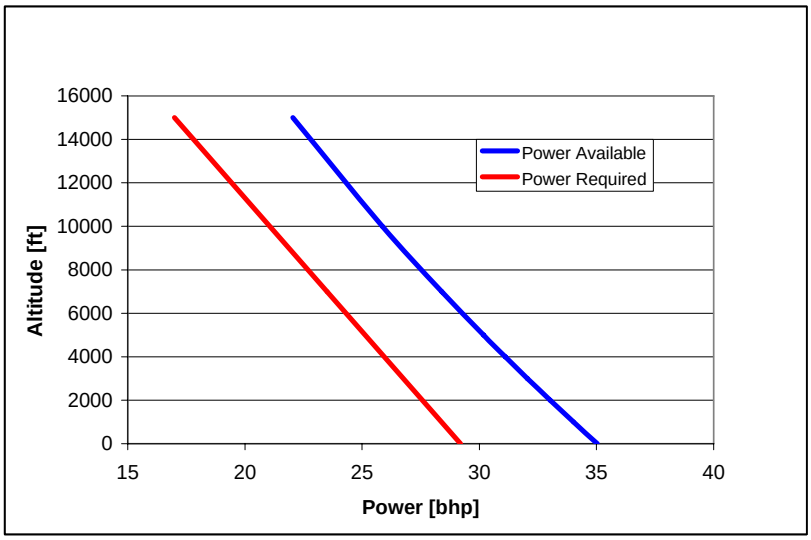

Figure 5-9. Available engine power vs. altitude.

Using the engine data as well as the desired flight velocities, a propeller was designed and optimized for the loiter conditions. Table 5-5 shows the results of the design of the two bladed propeller, which can expect to have an efficiency of 0.821, a number greater than early

expectations. Aluminum will be the material used because it produces greater propeller efficiency than a wooden propeller would.

Table 5-5. Propeller data.

C_Root [in]	2.5
Diameter [ft]	2.5
Advance Ratio	0.675
Coefficient of Power	0.083
Taper Ratio	0.52
Activity factor	80
Blades	2
Twist[deg]	22.5
Propeller Efficiency	0.821

6 Aerodynamics

Lift-to-drag performance as well as robustness of the airfoil determined airfoil selection of the aircraft. Three airfoil families make up the study group: the NACA 6-series, the NASA Natural Laminar Flow (NLF) series, and the Liebeck airfoils. All the airfoils studied are laminar flow airfoils meaning there is laminar flow over a significant portion of the airfoil. This allows for low drag, and good lift-to-drag characteristics. These airfoils are very sensitive to disturbances, but benefits vastly outweigh the downsides of these airfoils. The advantageous region for laminar flow the drag bucket; in this area, the drag drops below the expected lift-to-drag curve forming a "bucket" below the curve where the best performance is obtained.

The 6-series airfoil designs emerged in the 1940's making them dated designs. The Liebeck airfoils and NLF airfoils surfaced decades later, thus they have the benefit of more advanced technology. An increase in laminar flow results from using the more advanced airfoils leading to better performance. Figure 6-1 shows the drag polar of several of the selected airfoils. The team analyzed the airfoils using the XFOIL program at the design Mach number of .15.

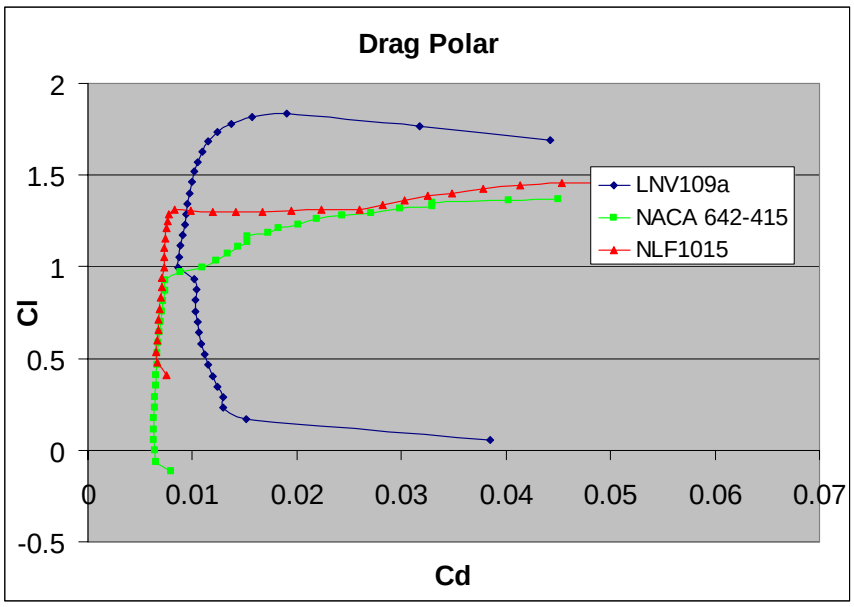

Figure 6-1. Drag polar of selected airfoils.

Next, the lift-curve slopes were studied to understand how the airfoils perform at different angles of attack. The NLF shows a peculiar lift-curve slope in that it flattens out at higher angle of attack but does not stall. The reason for this is the large amount of camber at the

trailing edge. This results in some trailing edge separation but not a full airfoil separation that leads to stall. Trailing edge stall causes the loss of some lift, but is not detrimental to the airfoil. This means that overall the airfoil provides a large range of angles of attack over which good lift results. Figure 6-2 shows the two other selected airfoils. The UAV will generally be at relatively low angles of attack for cruise. It will only use higher angles to turn and climb. The Liebeck shows a moderately normal lift-curve slope while the NACA airfoil ends in a very gentle slope at high angles of attack. This may indicate a soft stall, in other words minimal loss of lift during stall. For maximum lift, the Liebeck airfoil is superior, but many other factors were involved in selecting an airfoil.

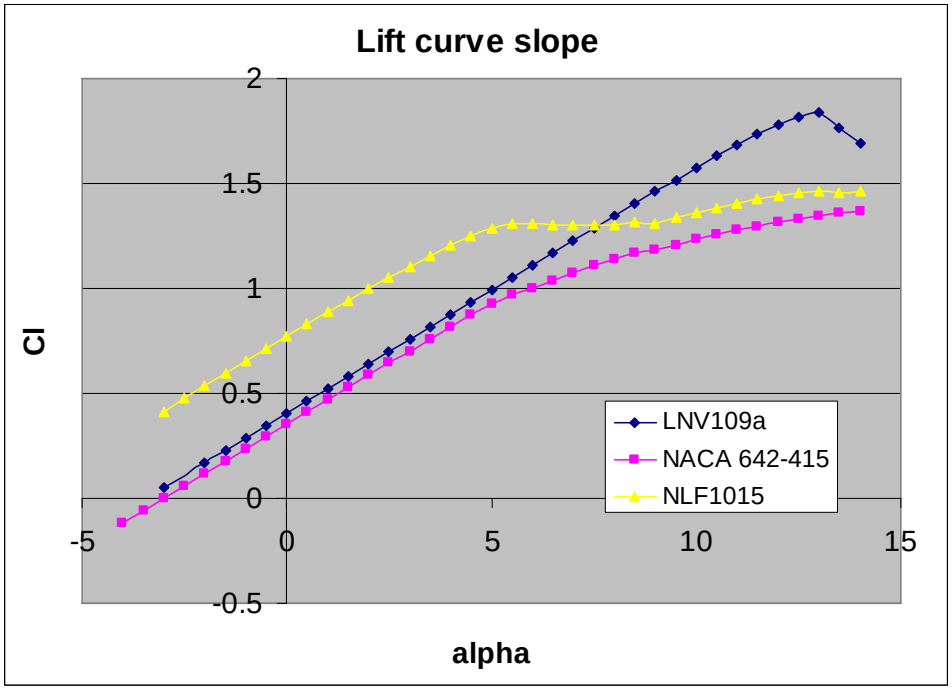

Figure 6-2. Lift-curve slope of several airfoils.

Next, lift-to-drag curves where compared for all the tested airfoils. This plot illustrates which airfoil is superior in each regime and what the final decision for airfoil selection is based on. The Liebeck and NLF airfoils show very good characteristics but in very different regimes. The NACA airfoil performs worse in every part of the regime studied. By either airfoil so it no longer considered in favor of one of the other airfoils.

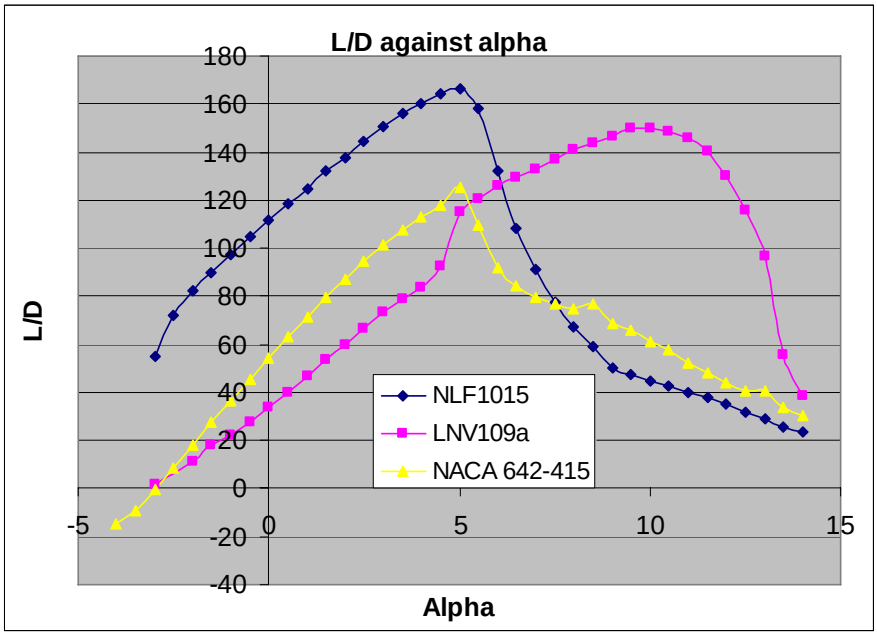

Figure 6-3. Lift-to-drag as a function of angle of attack.

The major difference between the Liebeck and NLF airfoils is where the peak performance occurs. Figure 6-3 shows the NLF having its peak performance at a lower angle of attack and the Liebeck having its peak at high angle of attack. This is the key factor in deciding which airfoil to choose. Since the airfoil operates at low angles of attack during the majority of the design mission, the superior lower angle of attack properties of the NLF was a major factor. The Liebeck requires flying at a high angle of attack so if maneuvering becomes necessary, only a limited amount angle of attack would be available in which to do so. The NLF allows larger amount of angle of attack with which to maneuver and became the main airfoil for the airplane.

The UAV will use flaps as a high lift device. This decreases the landing and takeoff speed of the aircraft that will also allow it to last longer because of the extra lift generated, in other words the extra lift with soften the impact on landing. Landing at a slower speed causes less wear and tear on the airframe. The wing section also has a slightly lower lift-to-drag maximum value than desired so the flaps will help raise that in cases where higher lift-to-drag becomes necessary. The wing does not institute the use of slats due to the minimal lift-to-drag change at higher angles of attack. Slats also add unnecessary weight that degrades the performance of the aircraft.

6.1 Drag Buildup

The parasite drag of the aircraft is a major factor in the overall drag buildup of the aircraft. Table 6-1 gives the component drag build up for the UAV. The equations from Raymer do not size an aircraft as small as this UAV so these values may be inaccurate. Form factors for various pieces were unknown, and as a result, more analyses on these pieces are necessary. The largest contributor to the parasite drag is the landing gear assembly. This is because even with a sleek fairing, the gear hanging in the free stream generates a large amount of drag.

Table 6-1 Component drag buildup

$C_{D,misc}$	0.003
$C_{D,landing}$	0.012
$C_{D,wing}$	0.006345
$C_{D,fus}$	0.0017
$C_{D,tail}$	0.002243
C_{Do}	0.0176

The drag polar of the aircraft is the final major part of conceptual aerodynamics. This shows how the aircraft will perform throughout its flight regime. The flapped drag polar is also explored as it is very important to know how the aircraft will perform with high lift devices deployed. Figure 6-4 shows the drag polar for the aircraft. It is flat for most of the regime because the drag "bucket" for the airfoil is very large. This means that at almost all angles of attack the drag is very low leading to the relatively flat curve.

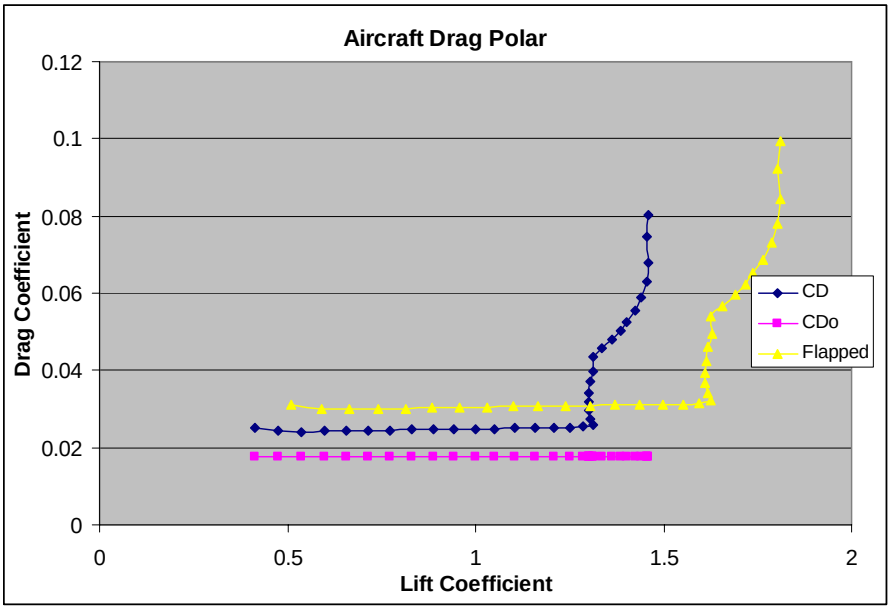

Figure 6-4. Aircraft Drag Polar

7 Stability and Trim

The team performed a stability analysis for this design to satisfy basic static stability requirements. A more thorough dynamic analysis is beyond the scope of this preliminary investigation; consequently, the methods used to obtain these results are largely rough approximations based on simplified models. The textbook by Raymer is the basis for these calculations.

7.1 Longitudinal Characterizations

Longitudinal effects taken into consideration in the design aircraft include all forces exerting moments about the center of gravity, summarized in Equation 7-1 below:

Equation 7-1. Moment about center of gravity.

$$M_{cg} = L\left(X_{cg} - X_{acw}\right) + M_w + M_{w\delta f}\delta_f + M_{fus} - L_h\left(X_{ach} - X_{cg}\right) + Tz_t + F_p\left(X_{cg} - X_p\right)$$

For an initial static stability analysis, the sum of the forces about the center of gravity must be zero. The terms above represent, in respective order: wing lift, wing twisting moment, wing twisting due to flap deflection, horizontal tail lift (assumed to act downwards), moment arm of the engine thrust, and moment arm of the vertical force produced at the propeller or intake disk due to the turning of the freestream airflow. The presented design has the engine mounted directly behind the center of gravity making the last two terms in that equation negligible. Furthermore, all the terms above simplify by expressing them in their non-dimensional coefficient forms. All lengths may be expressed as fractions of the wing mean chord (represented by $\overline{X}$), and the ratio between the dynamic pressure at the tail and the freestream dynamic pressure may be defined as η_h. These simplifications produce the driving equation for the longitudinal analysis, shown below as Equation 7-2:

Equation 7-2.

$$C_{m\,cg} = C_L\left(\overline{X_{cg}} - \overline{X_{acw}}\right) + C_{m\,w} + C_{m\,\delta\,f}\,\delta f + C_{m\,fus} - \eta_h \frac{S_h}{S_w} C_{L\,h}\left(\overline{X_{ach}} - \overline{X_{cg}}\right)$$

Defining the terms above may be accomplished using the estimations from tables in Raymer's chapter 16; these terms include the theoretical lift increment for plain flaps, an empirical correction for the plain lift increment, and the center of pressure for lift increment due to flaps. Combining Equation 7-2 with Equation 7-3 and Equation 7-4 shown below for the tail lift and total lift terms gives the elevator trim analysis for the UAV.

Equation 7-3.

$$C_{L\,h} = C_{L\,h\,\alpha}\left[\left(\alpha + i_w\right)\left(1 - \frac{\delta\varepsilon}{\delta\alpha}\right) + \left(i_h - i_w\right) - \alpha_{0L\,h}\right]$$

Equation 7-4.

$$C_{L\,total} = C_{L\,\alpha}\left[\alpha + i_w\right] + \eta_h \frac{S_h}{S_w} C_{L\,h}$$

To obtain a graphical solution, arbitrarily assumed angles of attack and elevator deflection angles provide the means to calculate the total-pitching-moment coefficient. This produces an elevator trim diagram, shown below as Figure 7-1. At cruise trim conditions of 100 kts, the resulting lift coefficient is approximately C_L = 0.45. This location on the line of zero cg-moment is one possible trim point for the aircraft design.

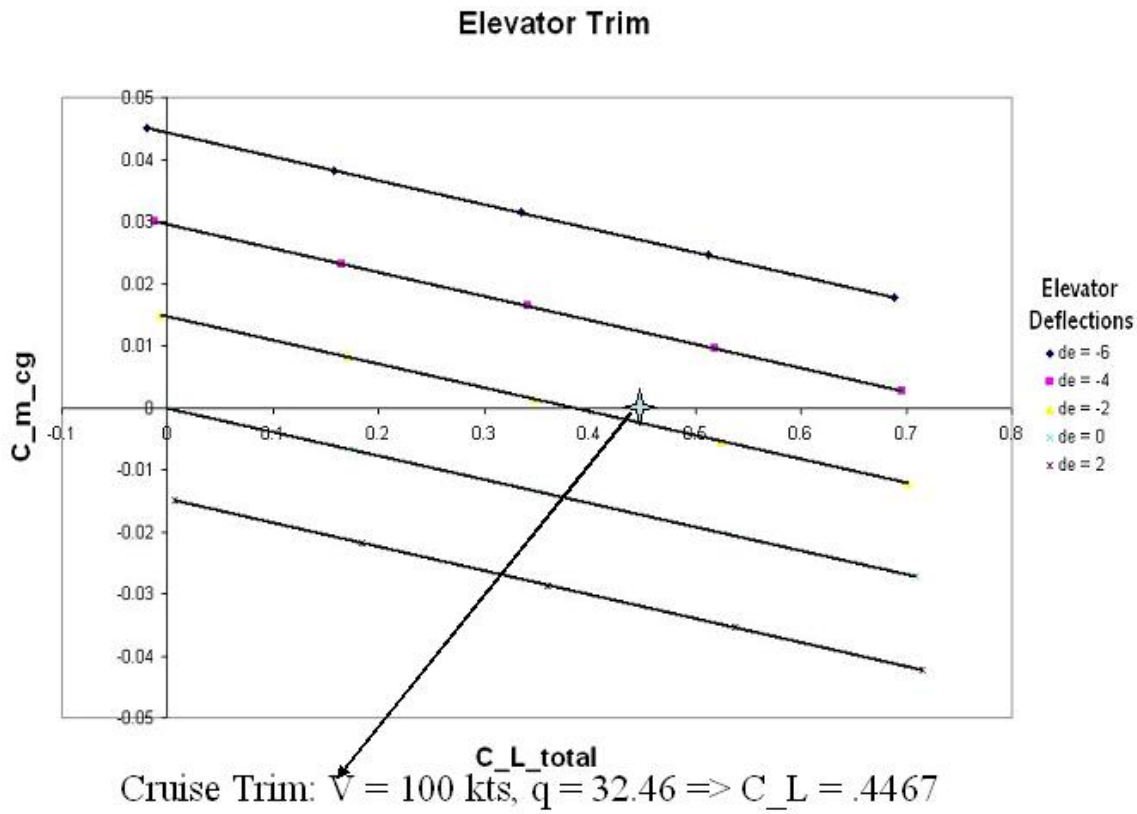

Figure 7-1: Elevator trim diagram

7.2 Lateral Characterizations

For the lateral trim analysis, commonly addressed trim conditions are aircraft operation with one engine out, and ability to operate in a crosswind. For the current analysis, as the engine-out condition is not an issue, control authority with a crosswind at 30% of the aircraft's takeoff velocity with 20 degrees of rudder deflection makes up the lateral trim analysis. An iterative process checks values from a simple sum of vectors resulting from the crosswind condition and the equation for the yaw-moment coefficient, Equation 7-6. The yaw moment is determined using methods presented in Raymer and derived from Equation 7-5 below.

$$N = N_{wing} + N_{w_{\delta a}}\delta_a + N_{fus} + F_v\left(X_{acv} - X_{cg}\right) - TY_p - DY_p - F_p\left(X_{cg} - X_p\right)$$

Equation 7-5

These terms represent, in respective order: the yaw moment from the wing, the yaw moment of the wing due to aileron deflection, the yaw moment of the fuselage, the force from the vertical tail, engine thrust, drag due to engine out, and vertical force due to turning at the propeller/intake disk. Due to the rear engine design of the aircraft, it is possible to neglect the last three terms of the equation. Expressing Equation 7-5 in non-dimensional form gives Equation 7-6.

$$C_n = C_{n\beta_w}\beta + C_{n\delta_a}\delta a + C_{n\,fus}\beta + C_{n\beta_v}\beta$$

Equation 7-6

$$C_{n\beta_v} = C_{F\beta_v}\frac{\partial\beta_v}{\partial\beta}\eta_v\frac{S_v}{S_w}\left(\overline{X}_{acv} - \overline{X}_{cg}\right)$$

Equation 7-7

Again, Raymer's textbook, chapter 16 facilitates defining and calculating the terms in these equations. The resulting iterations using the crosswind condition yield rough estimates for the rudder and aileron sizing, shown in Table 7-1:

Table 7-1. Control Surface Sizing

	Length [c/c_tot]	Flapped Area
Rudder/Elevator	0.8	2
Aileron	0.2	3
Flap	0.25	8

8 Performance

In order to approximate the performance of the UAV, the team uses values obtained from ACS to form a flight envelope and a load factor versus velocity plot, or V-n diagram. Several assumptions about the UAV's operating conditions allow for an accurate depiction of the UAV. For the purpose of the performance analysis, all calculations use conditions at cruise. During cruise, the aircraft operates at a mean altitude of 5000 ft MSL with a velocity of 100 knots. All calculations assume a weight estimation of 85% of the aircraft's gross takeoff weight in order to approximate conditions during the cruise. This is to account for the fuel burned up to this point and give a better approximation for wing loading, which is a value necessary in predicting the performance of the aircraft.

The flight envelope using MATLAB codes found in Appendix B and shown in Figure 8-1 is a plot of altitude versus velocity. It shows where the aircraft can physically operate and what its limitations are.

Equation 8-1. Excess Power

$$P_s = V\left[\frac{T}{W} - \frac{qC_{D_0}}{W/S} - n^2\frac{K}{q}\frac{W}{S}\right]$$

Equation 8-2. *Power at Altitude*

$$P_{alt} = P_{sl} * \left(p_{alt}/p_{sl}\right)$$

Equation 8-3. *Stall Velocity*

$$V_{stall} = \sqrt{\frac{2}{\rho} * \frac{W}{S} * \frac{1}{C_{l_{\max}}}}$$

Equation 8-1 is a formula to obtain excess power. Setting this equation equal to zero simulates the aircraft at steady level flight and, when plotted as a function of altitude and velocity, yields the flight envelope. In order to accomplish this, many parameters, such as thrust-to-weight and dynamic pressure must be represented as functions of altitude and velocity. Substitution of

Equation 8-2 and Equation 8-3 into Equation 8-1 achieves results for excess power as altitude and velocity increase.

As a general trend, the ascending curve on the left represents the stall speed at a given altitude. As this curve levels off, it gives the aircraft's ceiling. The curve then starts to decline as shown on the right side of Figure 8-1. The maximum velocity bounds the flight envelope on the right by maximum velocity at which the aircraft can operate for a given altitude. The two different curves (n=1 and n=2) represent the aircraft's performance at different load factors. As would be expected, the aircraft has significantly decreased performance, especially in ceiling, at an increased load factor. In order for the aircraft to fly, it must operate in the area enclosed by these set of curves. The dashed red lines show the operating conditions for the designed UAV. The intersection of these two lines occurs well within the constraints set by the flight envelope and meaning that the aircraft is able to perform at the operating conditions specified.

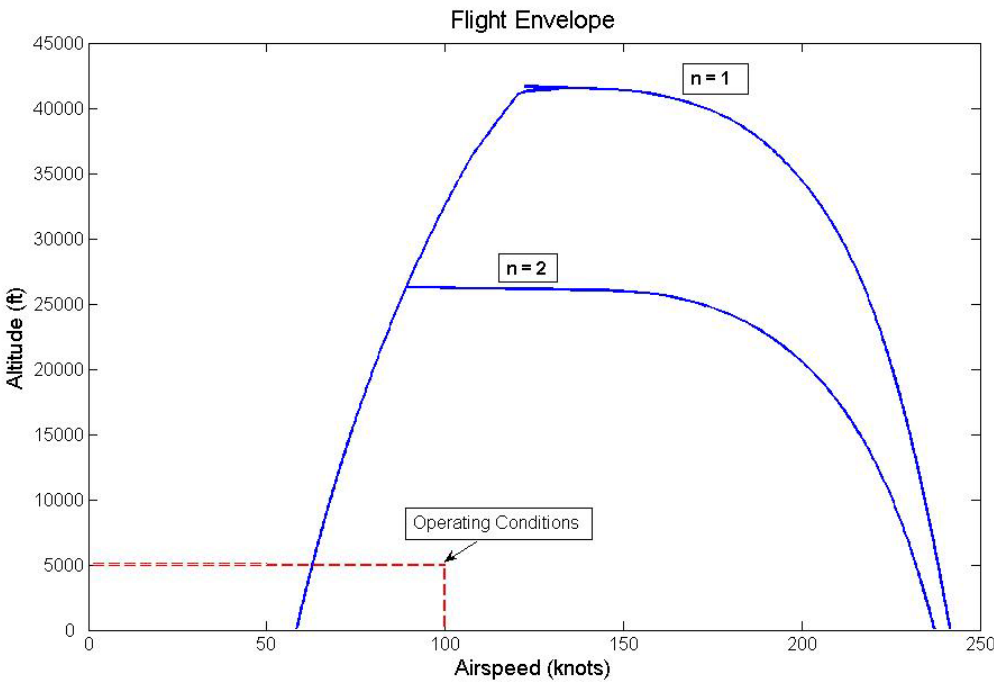

Figure 8-1. Flight Envelope.

Figure 8-2 shows the V-n diagram for the designed UAV. This plot is constructed using Both Equation 8-3 and Equation 8-4, which gives the load factor that the aircraft is undergoing during a maneuver, constrain the V-n diagram.

Equation 8-4. Load Factor.

$$n = \frac{\left(\frac{1}{2}\rho V^2 C_{l_{\max}}\right)}{W/S}$$

Again, the aircraft design is constrained to the area enclosed by the curve. The positive and negative parabolic curves located on the left of the diagram represent stall speed at a given load factor. The horizontal lines show velocity at a maximum designed load factor. The vertical line at the far right of the diagram illustrates a maximum velocity that the aircraft could structurally achieve. The operating conditions (steady level flight (n =1) and 100 knots) are represented by the dashed red lines in Figure 8-2 and are well within the constraining curves.

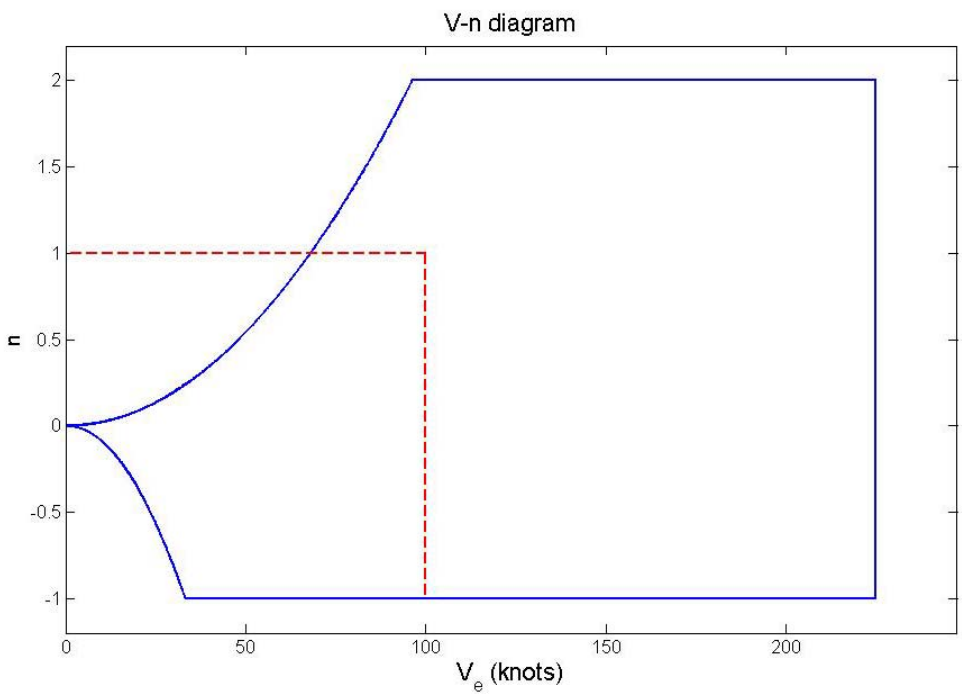

Figure 8-2. V-n Diagram.

Knowing that the aircraft can effectively operate at the specified conditions, additional computations yield more details about the aircraft's performance. Using Raymer's equations from chapters 5 and 17 gives values for takeoff and landing velocities as well as stall velocity. Table 8-1 shows these results. All calculated velocities use 5000 ft MSL as the altitude. The stall velocity calculated for the aircraft in mid cruise uses the approximation of 85% of the gross

take off weight. Takeoff velocity calculations assume a gross weight of 255 lbs and the landing velocity assumes zero fuel weight, resulting in a gross weight of 210 lbs. This results in the appropriate wing loading for these two values and gives a better estimation of the velocities. The landing and takeoff lengths were both outputs from ACS and take into account a 50 ft obstacle.

Table 8-1. Summary of Operating Velocities.

Operational Velocity	100 kts
Stall Velocity @ 5000 ft MSL and 85% GTOW	60 kts
Takeoff Velocity	75 kts
Landing Velocity	80 kts
Takeoff Dist	915 ft
Landing Dist	537 ft

9 Structures

An in depth study of the internal structural layouts of several UAVs in the database is performed to determine the structural properties of the designed UAV. Some of the characteristics desired from the UAV are the ability to operate in extreme loading conditions, excellent fatigue life, and corrosion resistance to ensure a long operating life. Trade studies of existing UAVs helped with material selection.

At this time, the team has created a conceptual design for the internal structural layout. Most UAVs with dimensions and aspect ratios similar to the team's UAV use a semi-monocoque design for the fuselage. The UAV fuselage, therefore, contains evenly spaced circular bulkheads and frames placed perpendicular to the longitudinal axis. The bulkheads and frames provide resistance to buckling and provide structural stability. Furthermore, in order to support axial loadings, longerons run along the longitudinal axis of the fuselage. This combination of longerons and bulkheads provides resistance to bending moments and increases the fuselage stiffness. The semi-monocoque ensures that the UAV will be structurally strong. Currently, the exact number of bulkheads remains an issue needing attention.

For the wing and the V-tail, two spars running parallel to the wing and tail become load-bearing tools. The reason for choosing spars is because the main load type experienced by the wing is lift distribution and the spars are excellent in distributing any forms of linear or non-linear lift force. The spar is also beneficial in supporting the V-tail against crosswind forces. For example, the Shadow 200, which also uses a V-tail, has three spars running longitudinally to resist crosswind forces. To help the wing and V-tail resist twisting, bending moments and torsional effects, evenly spaced ribs are used. I-beams along the airfoil also provide additional bending stiffness. Several UAVs, collected in the database, use this structural layout. One of the main concerns is that this configuration can increase structural weight if not designed properly. This is one of the main calculations needing completion.

In order to ensure selection of the most suitable material for the designed UAV, the team performed material properties analysis. For the wing and tail skin, AS4-3501 Carbon/Epoxy will be used. The spars and ribs of the wing and V-tail will also use the same material. Composites provide very high directional strength and have high fatigue life, resulting in its selection for the tail and wing skin. Furthermore, it allows for significant weight savings. This means that the

wing has the potential to handle any form of heavy load and can support the internal structural layout proposed for the wing without making it too heavy. Table 9-1 below gives the properties of several different commonly used composites [9].

Table 9-1. Elastic Moduli of Different Composites

Composite Type	E1(Msi)	E2(Msi)	G12(Msi)
S2 Glass/Epoxy	6.2	1.8	0.65
AS4/3501-6 (Carbon/Epoxy)	20	1.45	1
Kevlar-49/Epoxy	12.5	0.8	0.31
Boron/Epoxy	29	3	0.78
Boron/Aluminum	33.6	19.3	6.8

In Table 9-1, E_1 represents the Young's Modulus along the fiber, E_2 represents the Young's Modulus along the matrix and the G_{12} represents the shear modulus. Looking at this table, one can see that the composites with the highest strength are Boron/Epoxy, Boron/Aluminum and Carbon/Epoxy. The Boron composites were not chosen for the wing and tail skin despite their high strength properties. This is because it is very expensive to manufacture them. Furthermore, these composites do not have good fatigue resisting properties and they are not readily available in the market. On the other hand, Carbon/Epoxy is accessible from Boeing's facilities and any university that does composite research. It has a high Young's Modulus and the ability to resist chemical corrosion and has excellent fatigue life. Carbon/Epoxy can allow up to 25% weight savings over traditional metal alloys.

Unfortunately, the problem with composites is that it has high maintenance costs. Even though Carbon/Epoxy is cheaper than other composites, it is still much more expensive than metal alloys like aluminum. Since the fuselage contributes the most to the weight of the UAV but does not experience most of the lift force, the team determined not to select Carbon/Epoxy for the fuselage material because the overall production and maintenance cost of the UAV would be high. This results in the consideration of metal alloys. Studies of existing UAVs show that steel, aluminum and titanium are the most popular choices for the fuselage material. Figure 9-1 and Figure 9-2 represents strength to weight ratio and fracture toughness to weight ratios respectively [3].

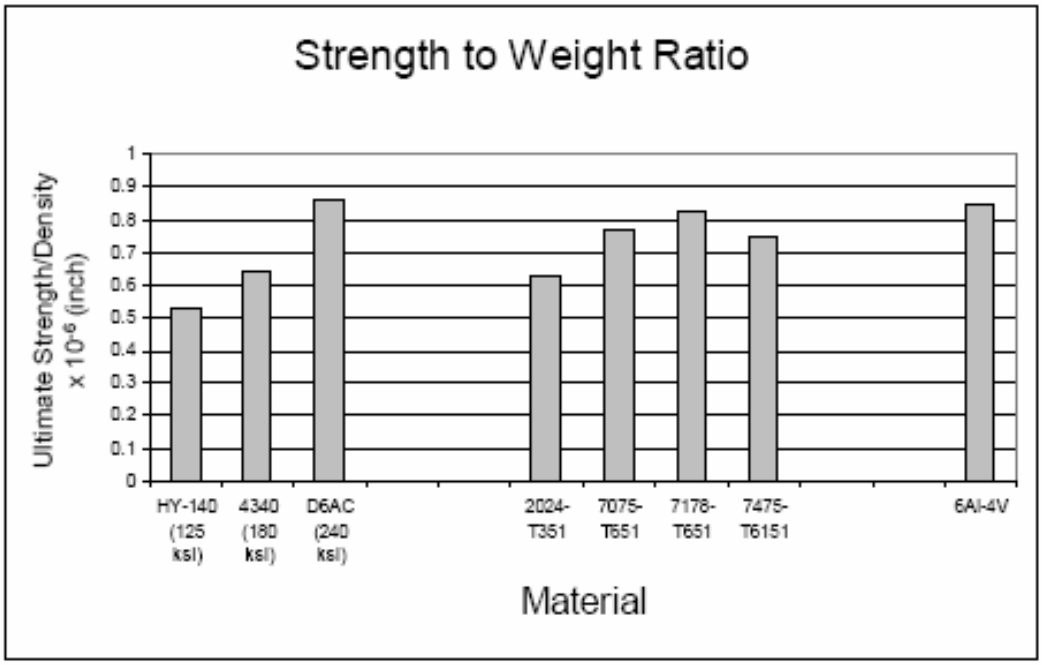

Figure 9-1. Strength to weight ratio of different alloys.

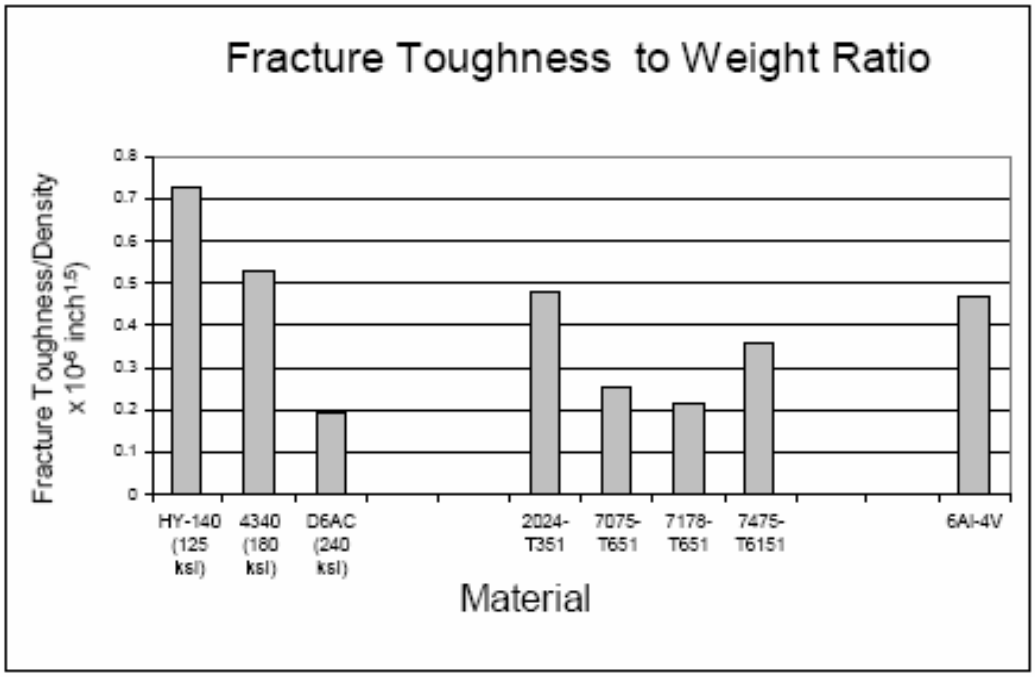

Figure 9-2. Fracture Toughness to Weight Ratio for Different Alloys.

In both these figures, the first three bars represent steel alloys, the middle four are for aluminum alloys and the last represents titanium alloy. The two figures show that steel alloys have very high strength to weight to ratio but poor fracture toughness ratio, with the exception of HY-140 steel. In addition, titanium 6A1-4V has very high strength and fracture toughness ratios. Despite HY-140 and 6A1-4V's high strength and fracture toughness ratios, these materials do not fit the fuselage's optimal design. Titanium is very expensive and difficult to maintain. Titanium's structural properties reduce significantly if it experiences any forms of impurities during manufacturing. Steel HY-140 has very poor corrosion resistance properties making it an inappropriate material selection. This leaves the aluminum alloys.

Looking at Figure 9-1 and Figure 9-2, Al-2024 has moderately high strength to weight ratio, with a Young's Modulus of 10e6 psi, and at the same time, a very high fracture toughness to weight ratio. Aluminum has additional benefits. It is very inexpensive. Currently, Al-2024 costs $3-4/lb (2) Furthermore, Al-2024 has excellent resistance to chemical corrosion. As a result, the fuselage and the boom material will use Al-2024 The spars, longerons, ribs and all the other internal structures will use Al-7075. This is because Al-7075 has a much higher strength to weight ratio than Al-2024. The main characteristic that the team wanted from the internal structure components was high strength to increase the UAV stiffness. The high

strength and moderate resistance to fracture of Al-7075 make it a suitable material for the internal structures of the UAV. Furthermore, Al-7075 can also allow for weight savings because it is much lighter than titanium and steel HY-140.

Material selection for the landing gear is also essential. Since the UAV will be landing and flying from extreme terrain, the landing gear needs high structural strength so that it can resist damages caused by impacts from the ground. Once again, Al-7075 is the material chosen for the landing gear. This is because Al-7075's high ultimate strength will make the landing gear resist potential damages caused by rough terrains in which the UAV will land on. In addition, using Al-7075 as the landing gear material will allow it to support the UAV body without causing quick fracture damage. Table 9-2 shows a summary of the material selection of all the components.

Table 9-2. Material selection of UAV components.

Component	Material
Wing	AS4-3501
V-tail	AS4-3501
Wing Ribs	AS4-3501
Wing Spar	AS4-3501
V-tail ribs/spars	AS4-3501
Fuselage/booms	Al-2024
Fuselage spars/longerons	Al-7075
Landing gear	Al-7075

One outstanding issue still needs more research. Since the wing and fuselage are made of different materials, a way to attach the two, without damaging the strength of the composite, needs to be determined. At this stage, two options are available. The first is to use a high strength adhesive to attach the wing and V-tail to the fuselage. The second is to use titanium root joints to attach the wing to the fuselage. The Eurofighter Typhoon uses this method of attaching its graphite composite wings to the aluminum fuel box, illustrating that the latter method has been successful before. Additional research will determine which way is the most suitable for joining composites and aluminum together for this UAV.

9.1 Weights and Balance

The primary method of obtaining a weight estimate for the designed UAV was to use the software ACS. The weight equations presented in Raymer's *Aircraft Design: A Conceptual Design* was also used to check if the values outputted by ACS were reasonable or not. Table 9-3

shows the complete list of all the component weights and Table 9-4 gives the overall summary of the aircraft weights.

Table 9-3. Weight buildup.

Empty Weight			Fuel		
Airframe Structures		**Weight(lbs)**	**Operating Items**		**Weight(lbs)**
Wing		25	Unusable Fuel &Oil		1
Fuselage		25	Fuel		39
V-Tail		8	**Total**		40
Nacelles		5			
Landing gear		7	**PAYLOAD**		
Total		70			**Weight(lbs)**
			Lidar		13
Propulsion		**Weight(lbs)**	CCNS		9
Engines		48	Camera		20
Fuel Systems		3	Installation		18
Total		51	**Total**		60
Fixed Equipments		**Weight(lbs)**			
Hydraulics		3			
Electrical		15			
Avionics		12			
Flight Controls		5			
Total		35			

Table 9-4. Component weight summary.

Component Summary	Weight(lbs)
Empty Weight	155
Fuel	40
Installed Payload	60
Total	255

In order to verify that this weight estimate was reasonable, it is compared with existing UAV weights. The existing UAV database showed that UAVs with similar dimensions had weights ranging from 200-350 lbs. For example, the Blue Horizon 2, which is around 10 ft in length, weighs 306 lbs [6]. The team's designed UAV's weight falls within 200-350 lbs, illustrating that the weight estimate outputted by ACS is realistic.

After obtaining the component weights, the center of gravity of the UAV is located. The calculation of the center of gravity is important because it helps in determining the stability of the aircraft. The center of gravity can be found using Equation 9-1.

Equation 9-1. Center of gravity

$$Xcg = \frac{W_i X_i}{W_t}$$

In Equation 9-1, W_i is the component weight, X_i is the component midpoint and W_t is the total weight. Table 9-5 below gives the component locations measure from the nose the aircraft. Equation 5 gave a center of gravity value of 3.649 ft from the nose of the UAV.

Table 9-5. Center of Gravity of Components

Component	Xi(ft)	XiWi
Wing	3.575	89.375
Fuselage	3.08	77
H.Tail	8.475	67.8
V.Tail	8.475	67.8
Landing gear	4.133	50
Engine	4.65	223.2
Fuel System	3.575	10.725
Fuel	3.575	142
Electrical	1.545	23.15
Avionics	1.545	18.54
LIDAR	2.1	27.3
CCNS	2.235	20.12
Camera	0.6	12
Booms	6.5	26

10 Reliability and Maintainability

As the design portion of products' lifecycle nears completion, and the gravity of the financial burden becomes apparent, the customer will want the satisfaction of knowing their product will be reliable and maintainable. Within each portion of the aircraft, there are characteristics that either highlight reliability or maintainability. From a structures standpoint, the aircraft performs minimal high performance maneuvers, keeping low stress on the ends of the wings. The absence of high stress leads to a lower stress fraction rate, which ultimately makes the aircraft more reliable. As mentioned earlier, from an aerodynamic perspective the static margin does not fluctuate with any great distance throughout the mission of the UAV, also making the vehicle reliable and easy to maintain.

The payload, discussed in Section 3, emphasized the capabilities of the UAV, however, because of the sensor packaging, the customer also receives highly reliable data with maintainable parts. Currently, the entire payload package is located in the front of the UAV, repressing the vibrations and movements from the engine positioned in the rear of the aircraft. This allows the data retrieved to be heavily relied on, and a second outside source obsolete. Finally, with the sensor package being small and with few parts, the maintainability of UAV easier and more cost effective.

11 Cost Analysis

When a product's life-cycle is discussed, the design teams and engineering groups are generally referring to the technical portions of the system with details such as performance, reliability, and even shelf life and storage. However, a product's affordability and total cost of the system, or life-cycle cost, (LCC) is often overlooked as the project nears its design completion. To avoid this potential disaster, it is beneficial to break down the different aspects of the total system value. These categories include design and development costs, construction and production costs, operation and maintenance costs, retirement costs, and material disposal costs. Many systems use cost estimating relationships (CER) to output various types of labor hours that convert to cost by multiplying by the appropriate hourly rate. The following section contains a detailed analysis of the cost break down for the UAS.

11.1 Cost-Estimating Methods

For this design project, a modified version of the Development and Procurement Costs of Aircraft IV (DAPCA IV) model approximates the various costs for the UAS. This original CER was developed to provide results for several classes of aircraft including bombers, transports, and cargo planes; for this analysis, an implemented scaling factor allows for reasonable cost estimation for the unmanned aerial system. The modified DAPCA model for the UAS includes the Research, Development, Test, and Evaluation (RDT&E), the production cost, which consists of the airframe, engine, and avionics. This model is the use of ground support equipment and initial spares, as well as the operations and maintenance requirements of the aircraft. The model, however, does not include the disposal of the UAV at the end of its lifecycle.

The RDT&E took in factors such as engineering, tooling, manufacturing, and quality control hours as well as development support cost, flight test cost, manufacturing materials cost, and added the COTS engine price. Wrap rates were also used during this portion of the analysis. They include the direct salaries paid to employees, employee benefits, overhead and administrative costs. In addition, the aircraft tabulatations used constant 2006 dollars.

In order to scale the DAPCA IV model down to an appropriate level, two sets of UAV data tested the reliability of the computational code written in MATLAB. This data includes

gross weight, maximum velocity, and overall cost of the aircraft. These UAVs are the Shadow 200 and the Pioneer, which are similar in size and weight to the UAV concept. According to the outputs, the analysis was off the market value of the tested UAVs by a factor of 15. It is therefore safe to assume that scaling the numbers down by a factor of 15 will result in a reasonable output.

The production costs for this analysis include the airframe, engine, and avionics components of the UAV. A design tool found on the NASA website helped to estimate the airframe cost. This tool also helped obtain the engine price. The avionics, estimated to be 15% of the entire flyaway cost, added a significant contribution to the production cost. The operations and maintenance cost took into consideration the fuel and oil cost, as well as the two-man crew that would be required to operate the UAV for the customers' benefit and the training it would require to operate the UAV. Finally, a 2% insurance cost was added to the end of the operations cost.

In order to simulate a realistic design mission, the design team acted as the voice of the customer while using the Trans-Alaskan pipeline as a typical consumer for the UAS. Following this method, the UAV flies 1600 nm a day for roughly 10 hours. The UAV also makes use of two ground stations, equipped with operators, and one relay station to transmit the signal to the observers. Table 11-1 gives individual breakdowns for various portions of the UAS.

Table 11-1. Cost analysis breakdown.

Break Down	Cost
Production Cost	$50,000.00
Cost Aircraft Sold at	$62,600.00
Break Even Point	80 UAVs @ 5 years
Operation & Maintenance cost (per year)	$154,000.00
Operation Cost Per Day	$428.00
Cost Per Mile (1600 Miles of Pipeline)	$0.27

12 Conclusion

The result of the design and market analysis performed is a compact, robust unmanned aerial system well equipped for the intended objectives. The business plan shows that a demand exists for the provided capability. Customer attributes contributed to engineering characteristics that provide a foundation and starting point for the vehicle design. The payload established for the mission, LIDAR and Visual/IR sensors, allow in-depth analysis of terrain features as well as the fulfillment of the primary customer concerns regarding third-party interference. The conceptual design centers on this capability. Avid's ACS sizing code provides the backbone of the analysis, supplemented by numerous other sources and techniques. Aerodynamic and structural investigations show good results for control surface sizing, and provide good approximations of aircraft geometry and load placement. Research into off-the-shelf propulsion options shows a prime candidate to provide the necessary performance for the demands of the mission. These attributes demonstrate feasible economic potential in an accompanying cost analysis.Figure 12-1. Oculus Superne UAV rendering.

Table 12-1 summarizes some of the primary attributes of the concept generated. The table compares these results with target and threshold values developed near the beginning of the analysis. This reflects the progress made towards satisfying the initial customer requirements. Table 12-2 provides a summary of more important design characteristics and economic factors. Most current values meet or exceed intended targets; future work would further refine these results, giving an even more desirable product to the customer.

Table 12-1. Summary of primary UAV parameters.

Parameter	Targets	Threshold	Current
Gross Weight [lbs]	300	500	255
Payload Capability Installed [lbs]	30	50	60
Endurance [hrs]	24	12	14.4
Loiter Velocity [kts]	150	100	100
Stall Speed [kts]	30	40	60
Takeoff Length [ft]	500	1500	915
Operational Altitude [ft AGL]	1000	2000	1000
SFC at Cruise [lb/bhp/hr]	0.4	0.6	0.48

Table 12-2. Continued summary of design characteristics.

Range [n.m.]	1300
Aspect Ratio	10
Wing Loading [lbs/ft^2]	20.3
Wing Span [ft]	11
Power to Weight Ratio [hp/lb]	0.15
Price per Unit	$62,600
Yearly Operational Cost	$154,000

The current version of this UAS, shown in Figure 12-1, has the potential to be a strong contender in the aerospace industry. Research supports this potential, particularly for the three mission fields presented in this report. Demand exists to replace current options with designs that increase safety and reduce costs. The final concept presented is not a complete design, however; much work remains before moving forward. Designers must accomplish further in-depth analysis to present thorough structural and aerodynamic results. As these aspects of the aircraft are refined, a more accurate description of the cost analysis will follow. Current results encourage pursuit of these more aggressive efforts in research and development.

Unmanned aerial systems are becoming a more prevalent solution to an advancing technological world, with their fields of application as numerous as they are diverse. Many private and government industries recognize the potential savings in cost and increase in safety accompanying these innovations. Oculus Superne takes pride in being a leader in the UAV revolution and providing these capabilities to its customers.

Figure 12-1. Oculus Superne UAV rendering.

References

[1] Callister, W.D. *Materials Science and Engineering.* 6th Ed., Wiley & Sons, 2003.

[2] Cross, N., excerpts from "Design Methods", *Engineering Design Methods*, Wiley, New York, 1989, pp. 33-41.

[3] Gere, Richard. *Mechanics of Materials*. 2nd Ed., Thomson/Brooks/Cole Publishing, 2004.

[4] Ingenieur-Gesellschaft fur Interface mbH, "Litmapper", 2005 http://www.litemapper.com/

[5] Israel Aerospace Industries, "MiniPOP Electro-Optical StabilizedPayload", 2002, http://www.iai.co.il/Default.aspx?docID=34441&FolderID=16641&lang=en&res=0&pos=0

[6] "Israeli-Weapons." www.israeli-weapons.com

[7] Pugh, S., "Conceptual Design," *Total Design: Integrated Methods for Successful Product Engineering*, Addison-Wesley, 1991, pp. 67-100.

[8] Raymer, D., Aircraft Design: A Conceptual Approach, Fourth Edition, AIAA Education Series, 2004.

[9] Sun, C.T. *Mechanics of Composites and Laminates.* Purdue University, 2007.

Appendix A QFD

HOW																	
Empty Weight (lbs)																	
Payload Capability (lbs)																	
Number of Systems		+	+														
Endurance [hrs]		+															
Engine Efficiency		-			+												
Operational Altitude (ft AGL)			+														
Operational Speed (mph)			+														
Stall Speed (C_l max)							+										
T/O Length (ft)		+							+								
gps Accuracy (in)																	
Sense and Avoid Accuracy (ft)			+	+							+						
Number of Operators												-					
Time between Overhauls (hrs)										-							
Designed Life (flight hrs)														+			
Communication Relay Time (secs)			-														

HOW

			Importance	Empty Weight (lbs)	Payload Capability (lbs)	Number of Systems	Endurance [hrs]	Engine Efficiency	Operational Altitude (ft AGL)	Operational Speed (mph)	Stall Speed (C_l max)	T/O Length (ft)	gps Accuracy (in)	Sense and Avoid Accuracy (ft)	Number of Operators	Time between Overhauls (hrs)	Designed Life (flight hrs)	Communication Relay Time (secs)	Total	Blue Horizon 2
				-	-	-	+	+	-	+	-	-	+	+	-	+	+	-		
WHAT	Performance	Efficient Speed	5.0	1	3		1	9	1	9	3								135	-
		Continuous Coverage	9.0	1			9	9	3	1	1		1					1	234	+
		Operate in Mountainous Terrain	5.0						9	3		1	3	9				3	140	+
		Ability to follow lines, circle at reasonable rate	7.0			3			3	3	1		9						133	-
		All Weather Operation	7.0	3	3				3	1	1		3	1				9	168	-
		Autonomous Operation	7.0										9	9	3			1	154	-
	Maintenance & Training	Ease of Maintenance	5.0	3		9	1								1	9			115	S
		Low Maintenance Cost	7.0		3	9									1	9	3		175	+
		Upgradeable	1.0	1	3	3			3	1	3			1		1	9		25	+
		Setup with Minimal Labor	2.0	3		3						3		1	9				38	-
		Fits in a Truck/Easily Transported	3.0	9		1	1					1			9				63	S
		Little Training Required to Operate	3.0			3							1	1	9			1	45	S
		Little Training Required to Repair	3.0			3									3	3	3		36	S
	Mission & Operations	Quickly Alerts to Trouble	6.0										1					9	60	-
		Easy to Operate Manually	5.0										3	3	9			1	80	+
		Integrated System	3.0			1						1	3		1		1	9	48	-
		Robust t/o Capability	5.0	3			1			1	9	9							115	+
		Able to See and Avoid Obstacles	6.0										3	9					72	S
		Low Environmental Impact (noise, pollution)	4.0				1	3	3	1		1							36	S
		Low Operational Cost	7.0	9	9		3	9			1	3	3	3	9		1	1	357	+
		Importance (Absolute)		162	123	162	124	201	134	107	93	87	243	211	225	118	49	190		
		Improtance (Relative)		7.3%	5.5%	7.3%	5.6%	9.0%	6.0%	4.8%	4.2%	3.9%	10.9%	9.5%	10.1%	5.3%	2.2%	8.5%		
		Targets		300	50	20	24	0.9	1000	150	30	500	4	1	2	2000	40000	5		
		Thresholds		500	30	30	12	0.6	2000	100	40	2001	20	5	4	750	28000	10		
		Current		306	42	-	16	0.8	1000	100	-	800	4	-	-	-	-	-		

Appendix B MATLAB Code

‘Env_fun.m’

```
function [Ps]=env_fun(V,h,n)
% h=x.h;
% n=x.n;
%n=1; % load factor
hp=40 - 100/18000 * h;   % power lapse from Fig 5.2 Raymer
prop_eff=.824;
weight=255*.85;
cd0=.0176;
area=12.55;
W_s=weight/area;
a=10;
oswald=.8;

[temp,press,rho,Hgeopvector]=atmosphere4(h,0);
[temp0,press0,rho0,Hgeopvector0]=atmosphere4(0,0);
k=1/(pi*a*oswald); % k
hp=40*press/press0;

q=.5.*rho.*V.^2;

TtoW=((550.*prop_eff)./V)*(hp./weight);
term2=(q.*cd0)./W_s;
term3=n^2.*(k./q).*W_s;
Ps=V.*(TtoW-term2-term3);
```

‘Flight_envelope.m’

```
clear; clc; close all;
h=100:200:50000;
service_ceiling=20000
v_fps_l(1) = fzero(@(x) env_fun(x,h(1),1),5);
V_s(1) = V_Stall(h(1));
v_fps_h(1) = fzero(@(x) env_fun(x,h(1),1),300);
for i=2:length(h)
    v_fps_l(i) = fzero(@(x) env_fun(x,h(i),1),v_fps_l(i-1));
    V_s(i) = V_Stall(h(i));
    v_fps_h(i) = fzero(@(x) env_fun(x,h(i),1),v_fps_h(i-1));
end
for count=1:length(v_fps_l)
    if (v_fps_h(count)-v_fps_l(count))>1E-1
        check(count)=0;
    end
    if v_fps_h(count)-v_fps_l(count)<1E-1
        check(count)=1;
    end
end
index=find(check,1,'first');
v_knots_l=max(v_fps_l.*0.5924838, V_s / 1.688);
v_knots_h=v_fps_h.*0.5924838;
plot(v_knots_l(1:index),h(1:index))
hold on;
```

```
v_knots_h(index)=v_knots_l(index);
plot(v_knots_h(1:index),h(1:index))
xlabel('Airspeed (knots)')
ylabel('Altitude')
title('Flight Envelope')



v_fps_l_2(1) = fzero(@(x) env_fun(x,h(1),2),5);
V_s_2(1) = V_Stall(h(1));
v_fps_h_2(1) = fzero(@(x) env_fun(x,h(1),2),300);
for i=2:length(h)
    v_fps_l_2(i) = fzero(@(x) env_fun(x,h(i),2),v_fps_l_2(i-1));
    V_s_2(i) = V_Stall(h(i));
    v_fps_h_2(i) = fzero(@(x) env_fun(x,h(i),2),v_fps_h_2(i-1));
end
count=0;
for count=1:length(v_fps_l_2)
    if (v_fps_h_2(count)-v_fps_l_2(count))>1E-10
        check_2(count)=0;
    end
    if v_fps_h_2(count)-v_fps_l_2(count)<1E-10
        check(count)=1;
    end
end
index_2=find(check,1,'first');
v_knots_l_2=max(v_fps_l_2.*0.5924838, V_s_2 / 1.688);
v_knots_h_2=v_fps_h_2.*0.5924838;
plot(v_knots_l_2(1:index_2),h(1:index_2))
hold on;
v_knots_h_2(index_2)=v_knots_l_2(index_2);
plot(v_knots_h_2(1:index_2),h(1:index_2))

alt_Op=[0 5000];
alt=[5000 5000];
V=[100 100];
op_V=[0 100];
plot(V,alt_Op,'r--')
plot(op_V,alt,'r--')
```

'V_stall.m'

```
function [V_s]=V_Stall(h)

weight=255;
area=12.55;
W_s=weight/area;

CL_max = 1.5;  %clean   (estimate)
[temp,press,rho,Hgeopvector]=atmosphere4(h,0);

V_s = sqrt(2/rho * W_s * 1 / CL_max);
```

‘V_n_diagram.m’

```
clear
clc;
close all;

altitude=5000;

[temp,press,rho_alt,Hgeopvector]=atmosphere4(altitude,0);
rho_SL=0.002377;
sigma=rho_alt/rho_SL;
CLmax=1.5;
W_s=20.25;
CL_alpha=2*pi;
V_dive=225;
V_cruise=100;
max_n=2;
%% Maneuver Loads
velocity_a=0:.1:500;
Ve_a=sigma.*velocity_a;
Ve_afps=1.68781.*Ve_a;
n_a=(0.5.*rho_alt.*Ve_afps.^2.*CLmax)./W_s;
plot(Ve_a(1:find(n_a>max_n,1,'first')),n_a(1:find(n_a>max_n,1,'first')))
hold on;
axis([0 V_dive*1.1 -1.2 max_n*1.1]);

Ve_b=[Ve_a(find(n_a>max_n,1,'first')) V_dive];
n_b=[max_n,max_n];
plot(Ve_b,n_b)

Ve_c=[V_dive V_dive];
n_c=[max_n,-1];
plot(Ve_c,n_c)

velocity_d=0:.1:150;
Ve_d=sigma.*velocity_d;;
Ve_dfps=1.68781.*Ve_d;
n_d=(0.5.*rho_alt.*Ve_dfps.^2.*CL_alpha)./W_s;
plot(Ve_d(1:find(n_d>1,1,'first')),-n_d(1:find(n_d>1,1,'first')))

 Ve_e=[Ve_d(find(n_d>1,1,'first')) V_dive];
 n_e=[-1,-1];
 plot(Ve_e,n_e)

xlabel('V_e (knots)')
ylabel('n')
title('V-n diagram')
 % ****** Operational Parameter *******
 Op_n=[1,1];
Op_speed = [V_cruise V_cruise]
speed=[0 100]
n=[-1,1]
plot(Op_speed, n,'r --')
plot(speed,Op_n,'r --')
```

‘atmosphere4.m’ (Written by Prof. Andrisani)

```
function [temp,press,rho,Hgeopvector]=atmosphere4(Hvector,GeometricFlag)
%function [temp,press,rho,Hgeopvector]=atmosphere4(Hvector,GeometricFlag)
% Standard Atmospheric data based on the 1976 NASA Standard Atmoshere.
% Hvector is a vector of altitudes.
% If Hvector is Geometric altitude set GeometricFlag=1.
% If Hvector is Geopotential altitude set GeometricFlag=0.
% Temp, press, and rho are temperature, pressure and density
% output vectors the same size as Hgeomvector.
% Output vector Hgeopvector is a vector of corresponding geopotential
altitudes (ft).
% This atmospheric model is good for altitudes up to 295,000 geopotential ft.
% Ref: Intoduction to Flight Test Engineering by Donald T. Ward and Thomas W.
Strganac
% index   Lapse rate   Base Temp     Base Geopo Alt        Base Pressure
Base Density
%   i     Ki(degR/ft)  Ti(degR)        Hi(ft)              P, lbf/ft^2
RHO, slug/ft^3
format long g
D= [1     -.00356616    518.67               0                   2116.22
0.00237691267925741
    2        0          389.97        36089.239          472.675801650081
0.000706115448911997
    3      .00054864    389.97        65616.798          114.343050672041
0.000170813471460564
    4      .00153619    411.57       104986.878          18.1283133205764
2.56600341257735e-05
    5        0          487.17       154199.475          2.31620845720195
2.76975106424479e-06
    6     -.00109728    487.17       170603.675          1.23219156244977
1.47347009326248e-06
    7     -.00219456    454.17       200131.234          0.38030066501701
4.87168173794687e-07
    8        0          325.17       259186.352        0.0215739175227548
3.86714900013768e-08];
R=1716.55;  %ft^2/(sec^2degR)
gamma=1.4;
g0=32.17405;    %ft/sec^2
RE=20926476;    % Radius of the Earth, ft
K=D(:,2);   %degR/ft
T=D(:,3);   %degR
H=D(:,4);   %ft
P=D(:,5);   %lbf/ft^2
RHO=D(:,6); %slug/ft^3
temp=zeros(size(Hvector));
press=zeros(size(Hvector));
rho=zeros(size(Hvector));
Hgeopvector=zeros(size(Hvector));

% Convert from geometric altitude to geopotental altitude, if necessary.
if GeometricFlag
    Hgeopvector=(RE*Hvector)./(RE+Hvector);
    disp('Convert from geometric altitude to geopotential altitude in feet')
else
   Hgeopvector=Hvector;
   %disp('Input data is geopotential altitude in feet')
```

```
end

ih=length(Hgeopvector);
n1=find(Hgeopvector<=H(2));
n2=find(Hgeopvector<=H(3) & Hgeopvector>H(2));
n3=find(Hgeopvector<=H(4) & Hgeopvector>H(3));
n4=find(Hgeopvector<=H(5) & Hgeopvector>H(4));
n5=find(Hgeopvector<=H(6) & Hgeopvector>H(5));
n6=find(Hgeopvector<=H(7) & Hgeopvector>H(6));
n7=find(Hgeopvector<=H(8) & Hgeopvector>H(7));
n8=find(Hgeopvector<=295000 & Hgeopvector>H(8));
icorrect=length(n1)+length(n2)+length(n3)+length(n4)+length(n5)+length(n6)+le
ngth(n7)+length(n8);
if icorrect<ih
    disp('One or more altitutes is above the maximum for this atmospheric
model')
    icorrect
    ih
end
% Index 1, Troposphere, K1= -.00356616
if length(n1)>0
    i=1;
    h=Hgeopvector(n1);
    TonTi=1+K(i)*(h-H(i))/T(i);
    temp(n1)=TonTi*T(i);
    PonPi=TonTi.^(-g0/(K(i)*R));
    press(n1)=P(i)*PonPi;
    RonRi=TonTi.^(-g0/(K(i)*R)-1);
    rho(n1)=RHO(i)*RonRi;
end

% Index 2,  K2= 0
if length(n2)>0
    i=2;
    h=Hgeopvector(n2);
    temp(n2)=T(i);
    PonPi=exp(-g0*(h-H(i))/(T(i)*R));
    press(n2)=P(i)*PonPi;
    RonRi=PonPi;
    rho(n2)=RHO(i)*RonRi;
end

% Index 3,  K3= .00054864
if length(n3)>0
    i=3;
    h=Hgeopvector(n3);
    TonTi=1+K(i)*(h-H(i))/T(i);
    temp(n3)=TonTi*T(i);
    PonPi=TonTi.^(-g0/(K(i)*R));
    press(n3)=P(i)*PonPi;
    RonRi=TonTi.^(-g0/(K(i)*R)-1);
    rho(n3)=RHO(i)*RonRi;
end

% Index 4,  K4= .00153619
if length(n4)>0
```

```
    i=4;
    h=Hgeopvector(n4);
    TonTi=1+K(i)*(h-H(i))/T(i);
    temp(n4)=TonTi*T(i);
    PonPi=TonTi.^(-g0/(K(i)*R));
    press(n4)=P(i)*PonPi;
    RonRi=TonTi.^(-g0/(K(i)*R)-1);
    rho(n4)=RHO(i)*RonRi;
end

% Index 5,  K5= 0
if length(n5)>0
    i=5;
    h=Hgeopvector(n5);
    temp(n5)=T(i);
    PonPi=exp(-g0*(h-H(i))/(T(i)*R));
    press(n5)=P(i)*PonPi;
    RonRi=PonPi;
    rho(n5)=RHO(i)*RonRi;
end

% Index 6,  K6= -.00109728
if length(n6)>0
    i=6;
    h=Hgeopvector(n6);
    TonTi=1+K(i)*(h-H(i))/T(i);
    temp(n6)=TonTi*T(i);
    PonPi=TonTi.^(-g0/(K(i)*R));
    press(n6)=P(i)*PonPi;
    RonRi=TonTi.^(-g0/(K(i)*R)-1);
    rho(n6)=RHO(i)*RonRi;
end

% Index 7,  K7= -.00219456
if length(n7)>0
    i=7;
    h=Hgeopvector(n7);
    TonTi=1+K(i)*(h-H(i))/T(i);
    temp(n7)=TonTi*T(i);
    PonPi=TonTi.^(-g0/(K(i)*R));
    press(n7)=P(i)*PonPi;
    RonRi=TonTi.^(-g0/(K(i)*R)-1);
    rho(n7)=RHO(i)*RonRi;
end

% Index 8,  K8= 0
if length(n8)>0
    i=8;
    h=Hgeopvector(n8);
    temp(n8)=T(i);
    PonPi=exp(-g0*(h-H(i))/(T(i)*R));
    press(n8)=P(i)*PonPi;
    RonRi=PonPi;
    rho(n8)=RHO(i)*RonRi;
end
```

‘Lat_trim.m’

```
%
% Lat Trim
%
% From Raymer Ch. 16
%
clear
close all
clc

de = 0;
alpha = 0;

da = 10;  % NOTE: For now this can only be an integer from 0-40
K_Arr = [...
    1 1 1 1 1 1 1 1 1 1 ...
    1.0 .99 .98 .96 .94 .91 .88 .85 .81 .77 ...
    .74 .72 .70 .68 .66 .64 .63 .62 .61 .60 ...
    .59 .58 .57 .56 .55 .54 .53 .52 .51 .50 .49];
K_f = K_Arr(da+1);
da = da*pi/180;

cf_c = .3;
c_Arr = .01:.01:.5;
LiftIncr_Arr = linspace(0,6,50);
I = -1;
for i = 1:50
    if (cf_c - c_Arr(i)) < .0001
        I = i;
    end
end
if I == -1
    disp('You suck.')
else
    LiftIncrCoeff = LiftIncr_Arr(I);
end

cf_ch = .4;
I = -1;
for i = 1:50
    if (cf_ch - c_Arr(i)) < .0001
        I = i;
    end
end
if I == -1
    disp('You suck.')
else
    LiftIncrCoeff_h = LiftIncr_Arr(I);
end

B = 11.5;
B = B*pi/180;
V_to = 73; % [kts]
```

```
V_to = V_to*1.68781; % [fps]
V_cross = .2*V_to;
V_e = V_cross/sin(B);

%-- Geometry
X_cg = 3.591293;
X_p = 5.6467;
c = 1.15;
Xbar_cg = X_cg/c; Xbar_p = X_p/c;
X_acv = 8.313;
Xbar_acv = X_acv/c;
b = 14;
S_w = 16;
S_h = 4.11/2;
S_a = 1.15*2;
Y_a = 5;
S_ref = 16+1.8*1.15; % S_w + FuselageDiam*Chord
S_f = 3;
S_fh = 1;
Z_wf = 0;
i_w = 0; i_h = 0;
Sweep = 0;
Sweep_h = 0;
HLSweep = 0;
HLSweep_h = 0;
D_f = .9;  % Fus. Depth [ft]
W_f = 1.8;  % Fus. Width [ft]
AR = 12;
n_h = .9;
n_v = .9;
rho = .0237;
q = .5*rho*V_e^2;


%-- Wing Lateral-directional Derivatives
LiftIncr_h = .9*LiftIncrCoeff_h*(S_fh/S_ref)*cos(HLSweep_h);
C_lah = 0.03;
C_la = .14;
alpha_0Lh = -.01;
delalpha_0Lh = -1*LiftIncr_h*de/C_lah;
alpha_0Lh = alpha_0Lh+delalpha_0Lh;
de_da = 0.4;
C_Lh = C_lah*((alpha+i_w)*(1-de_da)+(i_h-i_w)-alpha_0Lh);
C_L = C_la*(alpha+i_w)+n_h*S_h*C_Lh;
C_nbw = C_L^2/(4*pi*AR);

C_lda = 2*K_f*LiftIncrCoeff*Y_a*S_a*cos(HLSweep)/(S_w*b);
C_nda  = -.2*C_L*C_lda;

%-- Fuselage Derivatives
C_nbfus = -1.3*5.5*D_f^2/(S_w*b);

%-- Prop Contribution
A_in = 4*pi;
mdot = rho*V_e*A_in;
alpha_p = 5; alpha_p = alpha_p*pi/180;
```

```
F_p = mdot*V_e*alpha_p;

m = 100;
C_FbvArr = linspace(0,.5,m);
for i = 1:m
    C_Fbv = C_FbvArr(i);
    C_d = .001;
    D = .5*rho*q*C_d*S_w;
    F_v = D*cos(B) + V_e*cos(B);
    S_v(i) = F_v/(q*C_Fbv);

    SideslipDer = (1/n_v)*(.724+(3.06*S_v(i)/S_w)/(1+cos(Sweep))-
.4*Z_wf/D_f+.009*AR);
    C_nbv1 = 1/B*(-C_nbw*B-C_nda*da-C_nbfus*B)+F_p/(q*S_w)*(Xbar_cg-Xbar_p);
    C_nbv2 = -C_Fbv*SideslipDer*n_v*(S_v(i)/S_w)*(Xbar_acv-Xbar_cg);

    err(i) = abs(abs(C_nbv1-C_nbv2)/C_nbv2);
end

plot(C_FbvArr,err)
xlabel('Tail Lift Coefficient'); ylabel('Error')

ERR = 10000;
for i = 1:m
    if err < ERR
        ERR = err;
        I = i;
    end
end

Tail = S_v(I)

'aae451cdnaught.m'
Re=964000;
xc=.4;
tc=.15;
M=.15;
Cf=.455/(log(Re)^2.58*(1+.144*M^2)^.65)
Sref=12;
ffus=5.5/sqrt(4/pi*1.45)
FFfus=1+60/ffus^3+ffus/400
Swetfus=20.82
Qfus=1;
fwing=1.15/sqrt(4/pi*.566)
FFwing=(1+.6/.4*.15+100*.15^4)*(1.34*M^.18)
swetwing=12;
Qtail=1.08;
FFtail=(1+.6/.3*.10*100*.1^4)*(1.34*M^.18)
Swettail=5;

CDlanding=(.13/12+.05/12)*.8
CDmisc=(.13/12+.05/12)*.2
Cdwing=Cf*FFwing
Cdfus=Cf*FFfus*Swetfus/Sref
Cdtail=Cf*FFtail*Qtail*Swettail/Sref
CD0=Cdtail+CDmisc+Cdfus+Cdwing
```

‘aae451stripanalysis.m’

```
L=290;
rho=.00175;
V=168.78;
b=14.4;
y=linspace(0,b/2);
g2(1)=86.8;
A=0;
for i=1:99
    g1(i)=g2(i);
    g2(i+1)=g2(1)*sqrt(1-4*y(i+1)^2/b^2);
    A=(y(i+1)-y(i))/2*(g2(i+1)+g1(i))+A;
    hold on
    plot(y(i),g2(i),'k<')
end
A=2*A;
gammaTri=A*2/b;
c=linspace(gammaTri,0);
plot(y,c)

e=.7
q=25;
CL=L/(.5*rho*V^2*12)
CDi=CL^2/(pi*e*12)
alphaI=CL/(pi*e*12)
xlabel('Span Length')
ylabel('Vorticity')
title('Wing Lift Distribution')
```

‘Longtrim.m’

```
%
% Long Trim
%
% From Raymer Ch. 16
%
clear
close all
clc

%-- Input
alphArr = [0 5 10];
alphArr = alphArr.*pi/180;
deArr = [-2 0 2];
deArr = deArr.*pi/180;
n = length(alphArr);

df = 0;  % NOTE: For now this can only be an integer from 0-40
K_Arr = [...
    1 1 1 1 1 1 1 1 1 1 ...
    1.0 .99 .98 .96 .94 .91 .88 .85 .81 .77 ...
    .74 .72 .70 .68 .66 .64 .63 .62 .61 .60 ...
    .59 .58 .57 .56 .55 .54 .53 .52 .51 .50 .49];
K_f = K_Arr(df+1);
df = df*pi/180;

cf_c = .25;
c_Arr = .01:.01:1;
LiftIncr_Arr = linspace(0,10,100);
I = -1;
for i = 1:100
    if abs((cf_c - c_Arr(i))) < .0001
        I = i;
    end
end
if I == -1
    disp('You suck.')
else
    LiftIncrCoeff = LiftIncr_Arr(I);
end

cf_ch = .8;
I = -1;
for i = 1:100
    if abs((cf_ch - c_Arr(i))) < .0001
        I = i;
    end
end
if I == -1
    disp('You suck.')
else
    LiftIncrCoeff_h = LiftIncr_Arr(I);
end
```

```
%-- Geometry
X_cg = 3.591293;
X_acw = 3.787;
c = 1.15;
Xbar_cg = X_cg/c; Xbar_acw = X_acw/c;
X_ach = 8.313;
Xbar_ach = X_ach/c;
i_w = 0;
i_h = 0.001;
S_w = 16;
S_h = 2.7;
S_ref = S_w+1.8*1.15; % S_w + FuselageDiam*Chord
S_refh = S_h;
S_f = 8;
S_fh = 2.5;
Sweep = 0;
Sweep_h = 0;
HLSweep = 0;
HLSweep_h = 0;
AR = 12;
n_h = .7;

for i = 1:n
    de = deArr(i);
    for j = 1:n
        alpha = alphArr(j);
        %-- Lift Coefficients
        LiftIncr = .9*K_f*LiftIncrCoeff*(S_f/S_ref)*cos(HLSweep);
        C_la = .01; % Fig. 12.5
        alpha_0Lw = -4.71; alpha_0Lw = alpha_0Lw*pi/180;
        delalpha_0Lw = -1*LiftIncr*df/C_la;
        alpha_0Lw = alpha_0Lw+delalpha_0Lw;
        C_l = C_la*(alpha+i_w-alpha_0Lw);

        LiftIncr_h = .9*LiftIncrCoeff_h*(S_fh/S_refh)*cos(HLSweep_h);
        C_lah = 2; % Fig. 12.5
        alpha_0Lh = 0; alpha_0Lh = alpha_0Lh*pi/180;
        delalpha_0Lh = -1*LiftIncr_h*de/C_lah;
        alpha_0Lh = alpha_0Lh+delalpha_0Lh;
        de_da = .4;
        C_Lh = C_lah*((alpha+i_w)*(1-de_da)+(i_h-i_w)-alpha_0Lh);

        %-- Wing Pitching Moment
        C_m0 = -.0075;
        C_mw = C_m0*(AR*cos(Sweep)^2/(AR+2*cos(Sweep)));

        %-- Wing Pitching-Moment Increment due to Flaps
        Xbar_cp = 0.45;
        C_mwdf = K_f*LiftIncr*(Xbar_cp-Xbar_cg);

        %-- Fuselage Pitching Moment
        W_f = 1.8;
        L_f = 6.2;
        C_mfus = K_f*W_f^2*L_f/(c*S_w)*alpha;
```

```
        C_mcg(i,j) = C_l*(Xbar_cg-Xbar_acw) +...  % Eqn. 16.7
            C_mw +...
            C_mwdf*df +...
            C_mfus -...
            n_h*S_h/S_w*C_Lh*(Xbar_ach-Xbar_cg);% +...
        %     T/(q*S_w)*Zbar_t +...
        %     F_p/(q*S_w)*(Xbar_cg-Xbar_p);

        C_L(i,j) = C_la*(alpha+i_w)+n_h*S_h/S_w*C_Lh+1;  % Eqn. 16.30
    end
end

plot(C_L(:,1),C_mcg(:,1),'-x',C_L(:,2),C_mcg(:,2),'-x',C_L(:,3),C_mcg(:,3),'-
x')
legend('de = -2','de = 0','de = 2','Location','Best')
hold on
x = linspace(min(min((C_L))),max(max((C_L))),100);
plot(x,zeros(1,100),':')

xlabel('C_L_t_o_t_a_l'); ylabel('C_m_c_g')
```

Appendix C ACS Raw Output

```
AIRCRAFT SYNTHESIS ACS COPYRIGHT AVID LLC 4.1.10 020306
1    CARD IMAGES OF CONTROL DATA


     CARD                    IMAGE
0
       1)  $DATA BLOCK A
       2)  UAV 1
       3)  $DATA BLOCK B
       4)  1,4,1,7,,0,1
       4)          1         4         1         7                   0         1
       5)  $DATA BLOCK C
       6)  5,10,,2,2,0,,0
       6)          5        10                   2         2         0                   0
       7)  $DATA BLOCK D
       8)  0.01,,-0.01,0.001
       8)       0.01               -0.01     0.001
       9)  0.0010,0.0010,,0.02
       9)     0.0010    0.0010                0.02
      10)  $DATA BLOCK E - Minimize Gross Weight
      11)  2,1845,-1
      11)          2      1845        -1
      12)  $DATA BLOCK F
      13)  $ Max Body Diameter (BDMAX)----------------------
      14)  1.0,9.0,
      14)        1.0       9.0
      15)  $ Body Length (BODL)-----------------------------
      16)  5.0,60.0,
      16)        5.0      60.0
      17)  $ Wing Area (SWG)--------------------------------
      18)  10.0,2000.0,
      18)       10.0    2000.0
      19)  $ Aspect Ratio, Wing (ARWG)----------------------
      20)  8,20.0,
      20)          8      20.0
      21)  $DATA BLOCK G
      22)  $ Max Body Diameter (BDMAX)----------------------
      23)  1,162,1.
      23)          1       162        1.
      24)  $ Body Length (BODL)-----------------------------
      25)  2,173,1.
      25)          2       173        1.
      26)  $ Wing Area (SWG)--------------------------------
      27)  3,1390,1.
      27)          3      1390        1.
      28)  $ Aspect Ratio, Wing (ARWG)----------------------
      29)  4,156,1.
      29)          4       156        1.
      30)  $DATA BLOCK H
      31)  2
      31)          2
      32)  $DATA BLOCK I
      33)  $ Overall Aircraft Density (ACDEN)---------------
      34)  2249,2249,
      34)       2249      2249
      35)  5.0,,13.0,
      35)        5.0                13.0
      36)  $ Body Fineness Ratio (FRATIO)-------------------
      37)  553,553,
      37)        553       553
      38)  4.25,,20.0,
      38)       4.25                20.0
      39)  $ DATA BLOCK P
      40)  4,0
      40)          4         0
      41)  $ 1845 = Gross weight
      42)  $ 1723 = sea level static thrust
      43)  $ 1660 = thrust at top of climb
      44)  $ 2394 = propeller slip stream velocity
      45)  1845,1723,1660,2394,
      45)       1845      1723      1660      2394
```

```
 46)  $ DATA BLOCK Q
 47)  2549,11
 47)        2549        11
 48)  .20,.21,.22,.23,.24,.25,.26,.27,
 48)         .20       .21       .22       .23       .24       .25       .26       .27
 49)  .28,.29,.30,
 49)         .28       .29       .30
 50)  $DATA BLOCK R - Engine HP and Wing area
 51)  2372,7,1390,7
 51)        2372         7      1390         7
 52)  $DATA BLOCK S - G. Weight, Cr. Thrust, Cr. Q, Cr. Cd, Climb grad, Stall
 53)  1845,1661,1117,274,2245,1736
 53)        1845      1661      1117       274      2245      1736
 54)  $DATA BLOCK T - Engine HP
 55)  80.,90.,100.,110.,120.,130.,140.
 55)         80.       90.      100.      110.      120.      130.      140.
 56)  $DATA BLOCK U - Wing Area
 57)  130.,140.,150.,160.,170.,180.,190.
 57)        130.      140.      150.      160.      170.      180.      190.
 58)  $DATA BLOCK V
 59)  END
1    TITLE:
     UAV 1



     CONTROL PARAMETERS;
     CALCULATION CONTROL,                NCALC =    1
     NUMBER OF GLOBAL DESIGN VARIABLES,   NDV =    4
     NUMBER OF SENSITIVITY VARIABLES,     NSV =    1
     NUMBER OF FUNCTIONS IN TWO-SPACE,  N2VAR =    7
     NUMBER OF APPROXIMATING VAR.      NXAPRX =    0
     INPUT INFORMATION PRINT CODE,     IPNPUT =    0
     DEBUG PRINT CODE,                  IPDBG =    1


     CALCULATION CONTROL, NCALC
     VALUE   MEANING
       1     SINGLE ANALYSIS
       2     OPTIMIZATION
       3     SENSITIVITY
       4     TWO-VARIABLE FUNCTION SPACE
       5     OPTIMUM SENSITIVITY
       6     APPROXIMATE OPTIMIZATION



     * * OPTIMIZATION INFORMATION
     GLOBAL VARIABLE NUMBER OF OBJECTIVE          = 1845
     MULTIPLIER (NEGATIVE INDICATES MINIMIZATION) = -0.1000E-01

     CONMIN PARAMETERS (IF ZERO, CONMIN DEFAULT WILL OVER-RIDE)

     IPRINT  ITMAX   ICNDIR   NSCAL   ITRM   LINOBJ  NACMX1   NFDG
       5      10       0       2       2       0       6       0

      FDCH            FDCHM           CT              CTMIN
      0.10000E-01     0.00000E+00    -0.10000E-01     0.10000E-02

      CTL             CTLMIN          THETA           PHI
      0.00000E+00     0.00000E+00     0.00000E+00     0.00000E+00

      DELFUN          DABFUN          ALPHAX          ABOBJ1
      0.10000E-02     0.10000E-02     0.00000E+00     0.20000E-01

     DESIGN VARIABLE INFORMATION
     NON-ZERO INITIAL VALUE WILL OVER-RIDE MODULE INPUT
     D. V.     LOWER          UPPER         INITIAL
     NO.       BOUND          BOUND          VALUE          SCALE
       1     0.10000E+01    0.90000E+01    0.00000E+00    0.00000E+00
```

```
  2     0.50000E+01    0.60000E+02    0.00000E+00    0.00000E+00
  3     0.10000E+02    0.20000E+04    0.00000E+00    0.00000E+00
  4     0.80000E-01    0.20000E+02    0.00000E+00    0.00000E+00


DESIGN VARIABLES
      D. V.     GLOBAL    MULTIPLYING
ID     NO.     VAR. NO.     FACTOR
 1      1       162       0.10000E+01
 2      2       173       0.10000E+01
 3      3      1390       0.10000E+01
 4      4       156       0.10000E+01


CONSTRAINT INFORMATION

THERE ARE  2 CONSTRAINT SETS
      GLOBAL  GLOBAL  LINEAR      LOWER      NORMALIZATION      UPPER      NORMALIZATION
 ID   VAR. 1  VAR. 2    ID        BOUND         FACTOR          BOUND         FACTOR
  1   2249    2249       0      0.50000E+01    0.50000E+01    0.13000E+02    0.13000E+02
  3    553     553       0      0.42500E+01    0.42500E+01    0.20000E+02    0.20000E+02

TOTAL NUMBER OF CONSTRAINED PARAMETERS =    2




* * SENSITIVITY INFORMATION

PRINT CONTROL,            IPSENS =    0
NUMBER OF SENSITIVITY OBJECTIVES =    4

GLOBAL NUMBERS ASSOCIATED WITH SENSITIVITY OBJECTIVES
 1845 1723 1660 2394

         GLOBAL    NOMINAL
NUMBER  VARIABLE    VALUE      OFF-NOMINAL VALUES
   1    2549      0.20000E+00  0.2100E+00 0.2200E+00 0.2300E+00 0.2400E+00 0.2500E+00
                               0.2600E+00 0.2700E+00 0.2800E+00 0.2900E+00 0.3000E+00




* * TWO-VARIABLE FUNCTION SPACE MAPPING INFORMATION

PRINT CONTROL, IP2VAR =    0

GLOBAL VARIABLE NUMBERS ASSOCIATED WITH F(X,Y), M2VZ
 1845 1661 1117  274 2245 1736    0


GLOBAL VARIABLE NUMBER CORRESPONDING TO X, N2VX = 2372

VALUES OF X-VARIABLE
0.8000E+02  0.9000E+02  0.1000E+03  0.1100E+03  0.1200E+03
0.1300E+03  0.1400E+03


GLOBAL VARIABLE NUMBER CORRESPONDING TO Y, N2VY = 1390

VALUES OF Y-VARIABLE
0.1300E+03  0.1400E+03  0.1500E+03  0.1600E+03  0.1700E+03
0.1800E+03  0.1900E+03




* * ESTIMATED DATA STORAGE REQUIREMENTS

          REAL                          INTEGER
INPUT  EXECUTION  AVAILABLE     INPUT  EXECUTION  AVAILABLE
```

```
       66        66      5000          36        36      1000


     AIRCRAFT TYPE - GENAVI
1    TITLE:
     UAV 1


     AIRCRAFT TYPE - GENAVI



     CONTROL PARAMETERS:
     READ CONTROL,                      MREAD =    5
     EXECUTION CONTROL,                 MEXEC =    3
     WRITE CONTROL,                    MWRITE =    5
     NUMBER IDENTIFYING CONVERGENCE
       VARIABLE FOR CONVERGED VEHICLE,   IOBJ = 1830
     NUMBER IDENTIFYING COMPARISON
       VARIABLE FOR CONVERGED VEHICLE,   JOBJ = 1845
     SUMMARY OUTPUT PRINT CODE,         IPSUM =    0
     GLOBAL ERROR PRINT CODE,          KGLOBP =    0
     GLOBAL COMMON INITIALIZATION CODE,  INIT =    0
     DEBUG PRINT CODE,                  IPDBG =    1
     GLOBAL PLOT CONTROL,               IGPLT =    0
     DATA TRANSFER INFORMATION FILE, IRDDTR   =    7
     DATA TRANSFER INFORMATION PRINT, IPDTR   =    0



     VEHICLE CONVERGENCE INFORMATION:
     CONVERGENCE TOLERANCE, TOL = 0.10000E-03
     ESTIM WCALC VS WEXT SLOPE  = 0.30000E+00
     BOUNDING WEIGHT, WGMAX     = 0.10000E+03




     MODULE IDENTIFICATION NUMBERS:

      NUMBER      MODULE
         1       GEOMETRY
         2       TRAJECTORY
         3       AERODYNAMICS
         4       PROPULSION
         5       STABILITY AND CONTROL
         6       WEIGHTS
         7       STRUCTURES
         8       SONIC BOOM
         9       ECONOMICS
        11       SUMMARY OUTPUT
        14       TAKEOFF AND LANDING
        15       AGILITY


     MODULES ARE CALLED FOR INPUT IN THE FOLLOWING ORDER:
         1    2    3    4    6


     MODULES ARE CALLED FOR EXECUTION IN THE FOLLOWING ORDER:
         1    2    6


     MODULES ARE CALLED FOR OUTPUT IN THE FOLLOWING ORDER:
         1    2    4    6    3
\



  Input for Module #  1
  ****************************************************************************
```

```
\


  Input for Module #  2
  ******************************************************************************
\


  Input for Module #  3
  ******************************************************************************
\


  Input for Module #  4
  ******************************************************************************
\


  Input for Module #  6
  ******************************************************************************


 **MODULE 6 INPUT ERROR. AFMACH ZERO DEFAULT VALUE RESET TO .85.**


  ******************************************************************************

     ** Begin Vehicle Convergence **

     Estimated Gross Weight       =      90.0


     Calculated Gross Weight      =     249.6
     Slope of Wcalc vs. West line =       0.30
     Delta between Wcalc and West =     159.6

     Estimated Gross Weight       =     100.0
     Calculated Gross Weight      =     254.7

     ** End Vehicle Convergence **

      1 Convergence Iterations Required
  ******************************************************************************
\

  Output for Module #  1
  ******************************************************************************

 Fuselage Definition (Type 2)
          Nose Length..................   1.000
          Nose Fineness Ratio..........   1.000
          Constant Section Length......   0.500
          Afterbody Length.............   4.000
          Afterbody Fineness Ratio.....   4.000
          Overall Length...............   5.500
          Maximum Diameter.............   1.000
          Body Planform Area...........   4.654

 Fuselage Definition

     X       R       Area
   0.20    0.23      0.17
   0.25    0.27      0.23
   0.30    0.30      0.29
   0.35    0.33      0.34
   0.40    0.36      0.40
```

```
  0.45    0.38      0.46
  0.50    0.40      0.51
  0.55    0.42      0.56
  0.60    0.44      0.60
  0.65    0.45      0.65
  0.70    0.47      0.68
  0.75    0.48      0.71
  0.80    0.48      0.74
  0.85    0.49      0.76
  0.90    0.50      0.77
  0.95    0.50      0.78
  1.00    0.50      0.79
  1.05    0.50      0.79
  1.10    0.50      0.79
  1.15    0.50      0.79
  1.20    0.50      0.79
  1.25    0.50      0.79
  1.30    0.50      0.79
  1.35    0.50      0.79
  1.40    0.50      0.79
  1.45    0.50      0.79
  1.50    0.50      0.79
  1.70    0.51      0.81
  1.90    0.51      0.82
  2.10    0.51      0.83
  2.30    0.51      0.83
  2.50    0.51      0.83
  2.70    0.51      0.82
  2.90    0.51      0.80
  3.10    0.50      0.78
  3.30    0.49      0.75
  3.50    0.48      0.72
  3.70    0.46      0.68
  3.90    0.45      0.63
  4.10    0.43      0.58
  4.30    0.41      0.52
  4.50    0.38      0.46
  4.70    0.35      0.39
  4.90    0.32      0.32
  5.10    0.28      0.24
  5.30    0.23      0.17
  5.50    0.15      0.07
                   Fuselage
 Max. Diameter......     1.000
 Fineness Ratio.....     5.500
 Surface Area.......    14.987
 Volume............     3.336

\

 Dimensions of Planar Surfaces (each)

                        Wing  H.Tail  V.Tail  Canard   Units

 NUMBER OF SURFACES.     1.0     1.0     1.0     1.0
 PLAN AREA..........    12.6     1.9     1.6     0.0 (SQ.FT.)
 SURFACE AREA.......    25.3     2.1     2.4     0.0 (SQ.FT.)
 VOLUME............     1.2     0.1     0.1     0.0 (CU.FT.)
 SPAN..............  11.203   3.104   2.330   0.000 (FT.)
 L.E. SWEEP.........   0.000   0.000   0.000   0.000 (DEG.)
 C/4 SWEEP..........  -0.637  -0.603  -0.431   0.000 (DEG.)
 T.E. SWEEP.........  -2.545  -2.411  -1.723   0.000 (DEG.)
 ASPECT RATIO ......  10.000   5.000   3.500   0.000
 ROOT CHORD.........   1.245   0.653   0.701   0.000 (FT.)
 ROOT THICKNESS.....   1.792   0.941   1.009   0.000 (IN.)
 ROOT T/C ..........   0.120   0.120   0.120   0.000
 TIP CHORD..........   0.996   0.588   0.631   0.000 (FT.)
 TIP THICKNESS......   1.434   0.706   0.908   0.000 (IN.)
 TIP T/C ...........   0.120   0.100   0.120   0.000
 TAPER RATIO .......   0.800   0.900   0.900   0.000
 MEAN AERO CHORD....   1.125   0.621   0.666   0.000 (FT.)
```

```
LE ROOT AT.........   1.339   4.847   4.799   0.000 (FT.)
C/4 ROOT AT........   1.650   5.010   4.975   0.000 (FT.)
TE ROOT AT.........   2.584   5.500   5.500   0.000 (FT.)
LE M.A.C. AT.......   1.339   4.847   4.799   0.000 (FT.)
C/4 M.A.C. AT......   1.620   5.002   4.966   0.000 (FT.)
TE M.A.C. AT.......   2.464   5.468   5.466   0.000 (FT.)
Y M.A.C. AT........   2.697   0.762   0.000   0.000
LE TIP AT..........   1.339   4.847   4.799   0.000 (FT.)
C/4 TIP AT.........   1.588   4.994   4.957   0.000 (FT.)
TE TIP AT..........   2.335   5.435   5.430   0.000 (FT.)
ELEVATION..........   0.500   0.000   0.000   0.000 (FT.)

GEOMETRIC TOTAL VOLUME COEFF  0.500   0.040   0.000
REQUESTED TOTAL VOLUME COEFF  0.500   0.040   0.000
ACTUAL TOTAL VOLUME COEFF     0.500   0.040   0.000

         E X T E N S I O N S
                              Strake   Rear Extension
Centroid location at.......      0.00      0.00
Area.......................      0.00      0.00
Sweep Angle................      0.00      0.00
Wetted Area................      0.00      0.00
Volume.....................      0.00      0.00

Total Wing Area............     12.55
Total Wetted Area..........     44.81

         F U E L   T A N K S
Tank        Volume    Weight   Density
Wing             1.       29.     50.00
Fus#1            0.       11.     63.78
Fus#2            0.        0.     50.00
Total                     40.

Mission Fuel Required          =        40. lbs.
Extra Fuel Carrying Capability =         0. lbs.
Available Fuel Volume in Wing  =         1. cu.ft.

Aircraft Weight  =    100.000 lbs.
Aircraft Volume  =      4.695 cu.ft.
Aircraft Density =     21.297 lbs./cu.ft.
Wing Fuel Volume - Total Fuel Volume Required =     -0.218 cu.ft.

ICASE = 4  (Fineness Ratio Method)
\

 Output for Module #  2
 ******************************************************************************

Trajectory Output

Mission  1  (PAYLOAD =     60. LB)

PHASE    M         H         CL      ALPHA    WFUEL    TIME    VEL
        SFC(I)  THRUST(I)    CD      GAMMA      W       WA      Q
        SFC(U)  THRUST(U)  CDINST     L/D    THR/THA    PR      X

WARM-UP           2000.                          0.2    5.00
        0.09        26.

TAKEOFF 0.05      2000.    2.3810   15.64       0.1    1.00     55.
        0.11        79.    0.5515   34.35      99.8    0.00      3.
        0.11        79.    0.0000    4.32      2.23    1.00    936.

2ND SEG 0.05      2400.    2.3810   15.64                       55.
        0.11         0.    0.5515   13.41      99.8    0.00      3.
        0.11        79.    0.0000    4.32      2.23    1.00

ACCEL   0.10      2000.    0.5765    4.06       0.0    0.02    111.
        0.12        72.    0.0296    0.00      99.6    0.00     14.
```

```
   Prop  0.00        72.    0.0000   19.47      1.00    0.00      0.

 CLIMB   0.14      5000.    0.2940    1.31       0.1    0.63    149.
         0.15        57.    0.0191   31.29      99.6    0.00     23.
   Prop  0.00        57.    0.0000   15.40      1.00    0.00      1.

 CRUISE  0.14      5000.    0.2307    0.76      36.8  856.61    154.
         0.49         5.    0.0179    0.00      62.8    0.00     24.
   Prop  0.00         5.    0.0000   12.90      0.10    0.00   1299.

 LANDING 0.04      2000.    2.3810   15.64                        44.
         0.09        23.    0.5525    7.46      64.8    0.00      2.
         0.09        23.    0.0000    4.31      0.30    1.00    538.

 Fuel Summary

 Total Fuel     =     40.     Takeoff Fuel:         Fuel Load:
   Mission Fuel =     37.         Warmup  =      0.     External =      0.
   Reserve Fuel =      2.         Takeoff =      0.     Internal =     40.
   Trapped Fuel =      1.

 Block Time                        =   14.388 hrs
 Block Range                       =   1300.0 n.m.
 Block Fuel                        =     37.2 lb.

 FAR Takeoff Field Length          =     936. ft   Factor = 1.00
 Landing Field Length (total run)  =     538. ft   Decel @ .300 Gs
 Landing Field Length (ground run) =      77. ft   Field Length Factor = 0.600
 Weight for Landing calculation    =      65. lbs
 Landing Thrust to Weight ratio    =    0.362
 Takeoff Weight                    =     100. lbs
 Landing Weight                    =      63. lbs
\

  Output for Module #  4
  ******************************************************************************
 Propulsion Output: Engine and Propeller

 Fixed Pitch Blade Angle Conditions
   Mach Number        0.1400
   Altitude           20000.

 Engine Type:Rotary Recipricating
   Sea Level Static HP (each)                   30.0
   Max. Shaft Speed (RPM)                    4500.00
   Multiplier for sfc                         0.6000
   Spcific D/Q (sq-ft/HP)                     0.0000
   Weight (lbs)                                 30.0

 Propeller Type                 HS Fixed Pitch
   Number of Blades                              2.
   Diameter (ft)                                2.50
   Chord (ft)                                   0.16
   Activity Factor                            100.00
   Integ. Lift Coef.                          1.0000
   Solidity                                   0.0815
   Tip Speed (ft/sec)                         589.04
   Power Loading (HP/ft**2)                     5.81
   Disk Loading (lb/ft**2)                      7.30
   Torque (ft lbs)                             33.26
   Velocity Slipstream (ft/sec)               107.34
   Multiplier for thrust                      1.0000
   Weight Scale Factor                        1.0000
   Weight (lbs)                                  5.2

 Gear Reduction                                                          Propeller Extrap.
Errors
   Engine/Propeller RPM Ratio                 1.0000                      1  Activity Factor
4  Ct
   Transmission Efficiency                    0.9500                      2  Advance Ratio
5  Cl integ.
```

```
   Auto. Trans. Shift Alt.                        0.                            3  Cp
6  Blade Angle
   Weight Scale Factor                        0.0100
   Weight (lbs)                                  0.0

 Propulsion System Weight/Engine               35.2
 Engine and Propeller Noise (PNdb)           82.765


 Mach Number = 0.00          Altitude      =       0.   Maximum RPM =    4343.

 Percent  HP/Eng  Gear  ThrustU  ThrustI  Bsfc   TsfcI  FFLOW  Tip   Advance   Prop     Cp
Ct    Blade  E
  Power           Loss                                          Mach   Ratio    effU
Angle  X
 -------  ------  ----  -------  -------  -----  -----  -----  ----  -------  ------  ------  ---
---  -----  -
  100.0%    29.2  -1.5      81.      81.  0.300  0.108    8.8  0.51   0.0000   0.285  0.1731
0.1664  28.96  0
   95.0%    27.3  -1.4      78.      78.  0.312  0.110    8.5  0.50   0.0000   0.292  0.1731
0.1664  28.96  0
   90.0%    25.4  -1.3      74.      74.  0.324  0.111    8.2  0.49   0.0000   0.299  0.1731
0.1664  28.96  0
   80.0%    21.6  -1.1      66.      66.  0.352  0.115    7.6  0.46   0.0000   0.315  0.1731
0.1664  28.96  0
   70.0%    17.8  -0.9      58.      58.  0.390  0.119    6.9  0.43   0.0000   0.336  0.1731
0.1664  28.96  0
   60.0%    14.0  -0.7      50.      50.  0.451  0.127    6.3  0.40   0.0000   0.365  0.1731
0.1664  28.96  0
   50.0%    10.4  -0.5      41.      41.  0.546  0.139    5.7  0.36   0.0000   0.403  0.1731
0.1664  28.96  0


 Mach Number = 0.15          Altitude      =    7000.   Maximum RPM =    4500.

 Percent  HP/Eng  Gear  ThrustU  ThrustI  Bsfc   TsfcI  FFLOW  Tip   Advance   Prop     Cp
Ct    Blade  E
  Power           Loss                                          Mach   Ratio    effU
Angle  X
 -------  ------  ----  -------  -------  -----  -----  -----  ----  -------  ------  ------  ---
---  -----  -
  100.0%    23.5  -1.2      50.      50.  0.372  0.176    8.8  0.54   0.8739   0.519  0.1374
0.1173  28.96  0
   95.0%    22.4  -1.1      50.      50.  0.381  0.171    8.5  0.54   0.8739   0.546  0.1374
0.1173  28.96  0
   90.0%    21.2  -1.1      50.      50.  0.389  0.166    8.2  0.54   0.8739   0.577  0.1374
0.1173  28.96  0
   80.0%    18.3  -0.9      44.      44.  0.415  0.171    7.6  0.52   0.9080   0.580  0.1349
0.1133  28.96  0
   70.0%    15.5  -0.8      39.      39.  0.448  0.180    6.9  0.50   0.9508   0.577  0.1312
0.1080  28.96  0
   60.0%    12.7  -0.6      33.      33.  0.496  0.192    6.3  0.47   1.0000   0.573  0.1259
0.1017  28.96  0
   50.0%    10.0  -0.5      27.      27.  0.566  0.212    5.7  0.45   1.0604   0.560  0.1181
0.0932  28.96  6


 Mach Number = 0.15          Altitude      =    7000.   Maximum RPM =    4500.

 Percent  HP/Eng  Gear  ThrustU  ThrustI  Bsfc   TsfcI  FFLOW  Tip   Advance   Prop     Cp
Ct    Blade  E
  Power           Loss                                          Mach   Ratio    effU
Angle  X
 -------  ------  ----  -------  -------  -----  -----  -----  ----  -------  ------  ------  ---
---  -----  -
  100.0%    23.5  -1.2      50.      50.  0.372  0.176    8.8  0.54   0.8739   0.519  0.1374
0.1173  28.96  0
   95.0%    22.4  -1.1      50.      50.  0.381  0.171    8.5  0.54   0.8739   0.546  0.1374
0.1173  28.96  0
```

```
   90.0%    21.2  -1.1      50.      50.  0.389  0.166    8.2  0.54   0.8739   0.577  0.1374
0.1173  28.96  0
   80.0%    18.3  -0.9      44.      44.  0.415  0.171    7.6  0.52   0.9080   0.580  0.1349
0.1133  28.96  0
   70.0%    15.5  -0.8      39.      39.  0.448  0.180    6.9  0.50   0.9508   0.577  0.1312
0.1080  28.96  0
   60.0%    12.7  -0.6      33.      33.  0.496  0.192    6.3  0.47   1.0000   0.573  0.1259
0.1017  28.96  0
   50.0%    10.0  -0.5      27.      27.  0.566  0.212    5.7  0.45   1.0604   0.560  0.1181
0.0932  28.96  6


 Mach Number = 0.17          Altitude      =    7000.   Maximum RPM =    4500.

 Percent  HP/Eng  Gear  ThrustU  ThrustI  Bsfc   TsfcI  FFLOW  Tip   Advance   Prop     Cp
Ct    Blade  E
  Power           Loss                                          Mach   Ratio    effU
Angle  X
 -------  ------  ----  -------  -------  -----  -----  -----  ----  -------  ------  ------  ---
---  -----  -
  100.0%    23.5  -1.2      45.      45.  0.372  0.194    8.8  0.54   0.9613   0.519  0.1302
0.1067  28.96  0
   95.0%    22.4  -1.1      45.      45.  0.381  0.189    8.5  0.54   0.9613   0.546  0.1302
0.1067  28.96  0
   90.0%    21.2  -1.1      45.      45.  0.389  0.182    8.2  0.54   0.9613   0.577  0.1302
0.1067  28.96  0
   80.0%    18.6  -0.9      43.      43.  0.409  0.177    7.6  0.53   0.9775   0.615  0.1285
0.1046  28.96  0
   70.0%    15.8  -0.8      37.      37.  0.440  0.186    6.9  0.51   1.0184   0.614  0.1237
0.0992  28.96  6
   60.0%    13.1  -0.7      32.      32.  0.481  0.198    6.3  0.49   1.0654   0.611  0.1174
0.0925  28.96  6
   50.0%    10.4  -0.5      26.      26.  0.546  0.219    5.7  0.46   1.1223   0.595  0.1089
0.0834  28.96  6


 Mach Number = 0.17          Altitude      =    7000.   Maximum RPM =    4500.

 Percent  HP/Eng  Gear  ThrustU  ThrustI  Bsfc   TsfcI  FFLOW  Tip   Advance   Prop     Cp
Ct    Blade  E
  Power           Loss                                          Mach   Ratio    effU
Angle  X
 -------  ------  ----  -------  -------  -----  -----  -----  ----  -------  ------  ------  ---
---  -----  -
  100.0%    23.5  -1.2      45.      45.  0.372  0.194    8.8  0.54   0.9613   0.519  0.1302
0.1067  28.96  0
   95.0%    22.4  -1.1      45.      45.  0.381  0.189    8.5  0.54   0.9613   0.546  0.1302
0.1067  28.96  0
   90.0%    21.2  -1.1      45.      45.  0.389  0.182    8.2  0.54   0.9613   0.577  0.1302
0.1067  28.96  0
   80.0%    18.6  -0.9      43.      43.  0.409  0.177    7.6  0.53   0.9775   0.615  0.1285
0.1046  28.96  0
   70.0%    15.8  -0.8      37.      37.  0.440  0.186    6.9  0.51   1.0184   0.614  0.1237
0.0992  28.96  6
   60.0%    13.1  -0.7      32.      32.  0.481  0.198    6.3  0.49   1.0654   0.611  0.1174
0.0925  28.96  6
   50.0%    10.4  -0.5      26.      26.  0.546  0.219    5.7  0.46   1.1223   0.595  0.1089
0.0834  28.96  6


 Propulsion was called                257 times.
 Engin routine was called             657 times.


\

  Output for Module #  6
  ******************************************************************************
```

Weight Statement - General Aviation
Based on data from K.D. Wood p A177

Qmax: 900.
Design Load Factor: 3.00
Ultimate Load Factor: 4.50
Structure and Material: Aluminum Skin, Stringer
Wing Equation: GASP Equation
Body Equation: GASP Equation

Component	Pounds	Kilograms	Percent	Slope	Tech	Fixed
Airframe Structure	77.	35.	30.09			No
Wing	25.	11.	9.76	2.81	1.00	No
Fuselage	25.	11.	9.71	2.00	1.00	No
Horizontal Tail (Low)	5.	2.	2.05	2.80	1.00	No
Vertical Tail	3.	1.	1.14	1.00	1.00	No
Nacelles	12.	5.	4.67	1.00	1.00	No
Landing Gear	7.	3.	2.76	2.20	1.00	No
Propulsion	49.	22.	19.39			No
Engines (1)	48.	22.	18.85	1.00	1.00	Yes
Fuel System	1.	1.	0.54	2.00	1.00	No
Fixed Equipment	29.	13.	11.23		1.00	No
Hyd & Pneumatic	1.	0.	0.20	1.00		No
Electrical	15.	7.	5.81	0.37		No
Avionics	8.	4.	3.18	0.30		No
Instrumentation	0.	0.	0.00	0.37		No
De-ice & Air Cond	0.	0.	0.00	0.00		No
Aux Power System	0.	0.	0.00	1.00		No
Furnish & Eqpt	0.	0.	0.00	0.00		No
Seats and Lavatories	0.	0.	0.00	0.00		No
Galley	0.	0.	0.00	0.00		No
Misc Cockpit	4.	2.	1.68	0.00		No
Cabin Finishing	4.	2.	1.37	0.00		No
Cabin Emergency Equip	0.	0.	0.00	0.00		No
Cargo Handling	0.	0.	0.00	0.00		No
Flight Controls	5.	2.	2.04	1.00		No
Empty Weight	155.	70.	60.71			
Operating Items	1.	0.	0.39			No
Flight Crew (0)	0.	0.	0.00			No
Crew Baggage and Provisions	0.	0.	0.00			No
Flight Attendents (0)	0.	0.	0.00			No
Unusable Fuel and Oil	1.	0.	0.39			No
Passenger Service	0.	0.	0.00			No
Cargo Containers	0.	0.	0.00			No
Operating Weight Empty	156.	71.	61.10			
Fuel	39.	18.	15.34			
Payload	60.	27.	23.56			Yes
Passengers (0)	0.	0.	0.00			No
Baggage	0.	0.	0.00			No
Cargo	0.	0.	0.00			No
Calculated Weight	255.	116.	76.44			No
Estimated Weight	100.	45.				
Percent Error			154.69			

Calculated Weight does not equal 100% because a group weight is being fixed.
\

Output for Module # 3

```
 ******************************************************************************

 Mach     =    0.05  C.G. Location =   1.6 ft, 0.20 cbar        Q =  3.7  Cj =  0.00 per engine
 Altitude =      0.  Takeoff Configuration:  Flaps and Slats    Thrust =       0. per engine

 Parasite Drag       Induced Drag
 Friction      .0183   Alpha    Cl     Cd  L/D   PF    e Zone  Cm  Cdtrim Deltrim StMrg
  Body         .0053     0.0 0.909 0.2296  4.0  3.8 0.12  1  0.004 0.0000     0.0 0.262
  Wing         .0104     2.5 1.148 0.2697  4.3  4.6 0.17  1  -.037 0.0000     0.0 0.268
  Strakes      .0000     5.0 1.385 0.3119  4.4  5.2 0.21  1  -.088 0.0000     0.0 0.274
  H. Tail      .0012     7.5 1.621 0.3575  4.5  5.8 0.25  1  -.154 0.0000     0.0 0.285
  V. Tail      .0014    10.0 1.858 0.4110  4.5  6.2 0.28  1  -.239 0.0000     0.0 0.300
  Canard       .0000    15.0 2.324 0.5342  4.4  6.6 0.33  1  -.450 0.0000     0.0 0.330
 Interference  .0006    30.0 3.599 1.0198  3.5  6.7 0.41  1  ***** 0.0000     0.0 0.000
  Base         .0000    45.0 2.714 0.9128  3.0  4.9 0.26  1  ***** 0.0000     0.0 0.000
  Wing-Body    .0003    60.0 1.365 1.5334  0.9  1.0 0.04  1  ***** 0.0000     0.0 0.000
  Wing-Nacelle .0000    75.0 0.572 ******  0.0  0.0 0.00  1  ***** 0.0000     0.0 0.000
  Excressence  .0003
 Wave          .0000
 External      .0000                      Slope Factors
  Tanks        .0000                        Cl/Alpha (per radian)       -0.2575
  Bombs        .0000                        Cdl/Cl^2                   ********
  Stores       .0000                      Alpha Transition Zone 2-3    115.240
  Extra        .0000
 Camber        .0004                      Flap Setting                     30.
 _________________                        Slat Setting                      0.
 Cdmin         .0193                      Flap Type        Single           1. sq. ft

 Mach     =    0.08  C.G. Location =   1.6 ft, 0.20 cbar        Q =  8.3  Cj =  0.00 per engine
 Altitude =      0.  Landing Configuration:  Flaps and Slats    Thrust =       0. per engine

 Parasite Drag       Induced Drag
 Friction      .0168   Alpha    Cl     Cd  L/D   PF    e Zone  Cm  Cdtrim Deltrim StMrg
  Body         .0049     0.0 0.909 0.2280  4.0  3.8 0.12  1  0.004 0.0000     0.0 0.262
  Wing         .0094     2.5 1.148 0.2682  4.3  4.6 0.17  1  -.037 0.0000     0.0 0.268
  Strakes      .0000     5.0 1.385 0.3103  4.5  5.3 0.21  1  -.088 0.0000     0.0 0.274
  H. Tail      .0011     7.5 1.621 0.3559  4.6  5.8 0.25  1  -.154 0.0000     0.0 0.285
  V. Tail      .0013    10.0 1.858 0.4094  4.5  6.2 0.28  1  -.239 0.0000     0.0 0.300
  Canard       .0000    15.0 2.324 0.5326  4.4  6.7 0.33  1  -.450 0.0000     0.0 0.330
 Interference  .0006    30.0 3.595 1.0160  3.5  6.7 0.41  1  ***** 0.0000     0.0 0.000
  Base         .0000    45.0 2.697 0.8941  3.0  5.0 0.26  1  ***** 0.0000     0.0 0.000
  Wing-Body    .0002    60.0 1.342 1.4917  0.9  1.0 0.04  1  ***** 0.0000     0.0 0.000
  Wing-Nacelle .0000    75.0 0.556 ******  0.0  0.0 0.00  1  ***** 0.0000     0.0 0.000
  Excressence  .0003
 Wave          .0000
 External      .0000                      Slope Factors
  Tanks        .0000                        Cl/Alpha (per radian)       -0.2701
  Bombs        .0000                        Cdl/Cl^2                   ********
  Stores       .0000                      Alpha Transition Zone 2-3     76.660
  Extra        .0000
 Camber        .0004                      Flap Setting                     30.
 _________________                        Slat Setting                      0.
 Cdmin         .0177                      Flap Type        Single           1. sq. ft
\
 Detailed Aerodynamics Output

 Mach     =    0.10  C.G. Location =   1.6 ft, 0.20 cbar
 Altitude =      0.  Reynolds Number per foot =    0.710x10^6

 Parasite Drag       Induced Drag
 Friction      .0158   Alpha    Cl     Cd  L/D   PF    e Zone  Cm  Cdtrim Deltrim StMrg
  Body         .0047     0.0 0.173 0.0175  9.9  4.1 0.62  1  0.006 0.0000     0.0 0.256
  Wing         .0088     2.5 0.422 0.0231 18.3 11.9 0.79  1  -.053 0.0000     0.0 0.265
  Strakes      .0000     5.0 0.671 0.0343 19.6 16.0 0.78  1  -.123 0.0000     0.0 0.275
  H. Tail      .0011     7.5 0.920 0.0512 17.9 17.2 0.76  1  -.206 0.0000     0.0 0.287
  V. Tail      .0012    10.0 1.168 0.0740 15.8 17.1 0.75  1  -.301 0.0000     0.0 0.298
  Canard       .0000    15.0 1.660 0.1369 12.1 15.6 0.73  1  -.523 0.0000     0.0 0.319
 Interference  .0005    30.0 3.029 0.4463  6.8 11.8 0.68  1  ***** 0.0000     0.0 0.000
  Base         .0000    45.0 2.450 0.4805  5.1  8.0 0.41  1  ***** 0.0000     0.0 0.000
  Wing-Body    .0002    60.0 1.278 1.2885  1.0  1.1 0.04  1  ***** 0.0000     0.0 0.000
  Wing-Nacelle .0000    75.0 0.536 1.7824  0.3  0.2 0.01  1  ***** 0.0000     0.0 0.000
```

```
 Excressence  .0003
Wave          .0000
External      .0000                      Slope Factors
 Tanks        .0000                        Cl/Alpha (per radian)        0.2775
 Bombs        .0000                        Cdl/Cl^2                     6.1451
 Stores       .0000                      Alpha Transition Zone 2-3     57.354
 Extra        .0000
Camber        .0004                      Programmed Flap Setting           0.
_________________
Cdmin         .0167                      Flap Type        Single           1. sq. ft

Mach     =    0.13  C.G. Location =   1.6 ft, 0.20 cbar
Altitude =      0.  Reynolds Number per foot =    0.887x10^6

Parasite Drag       Induced Drag
Friction      .0154   Alpha    Cl     Cd  L/D   PF    e Zone  Cm  Cdtrim Deltrim StMrg
 Body         .0046     0.0 0.142 0.0167  8.5  3.2 0.55  2  0.007 0.0000     0.0 0.236
 Wing         .0086     2.5 0.429 0.0228 18.8 12.3 0.81  2  -.055 0.0000     0.0 0.242
 Strakes      .0000     5.0 0.706 0.0353 20.0 16.8 0.80  2  -.127 0.0000     0.0 0.250
 H. Tail      .0010     7.5 0.974 0.0539 18.1 17.8 0.79  2  -.207 0.0000     0.0 0.258
 V. Tail      .0012    10.0 1.234 0.0783 15.8 17.5 0.77  2  -.296 0.0000     0.0 0.266
 Canard       .0000    15.0 1.730 0.1435 12.1 15.9 0.75  2  -.498 0.0000     0.0 0.279
Interference  .0005    30.0 3.028 0.4421  6.9 11.9 0.68  2  ***** 0.0000     0.0 0.000
 Base         .0000    45.0 3.297 0.6385  5.2  9.4 0.56  2  ***** 0.0000     0.0 0.000
 Wing-Body    .0002    60.0 0.568 1.8704  0.3  0.2 0.01  3  -.891 0.0000     0.0 0.000
 Wing-Nacelle .0000    75.0 0.210 2.0425  0.1  0.0 0.00  3  -.803 0.0000     0.0 0.000
 Excressence  .0003
Wave          .0000
External      .0000                      Slope Factors
 Tanks        .0000                        Cl/Alpha (per radian)        0.0520
 Bombs        .0000                        Cdl/Cl^2                    45.8417
 Stores       .0000                      Alpha Transition Zone 2-3     45.757
 Extra        .0000
Camber        .0004                      Programmed Flap Setting           0.
_________________
Cdmin         .0163                      Flap Type        Single           1. sq. ft
\
Detailed Aerodynamics Output

Mach     =    0.15  C.G. Location =   1.6 ft, 0.20 cbar
Altitude =      0.  Reynolds Number per foot =    1.065x10^6

Parasite Drag       Induced Drag
Friction      .0154   Alpha    Cl     Cd  L/D   PF    e Zone  Cm  Cdtrim Deltrim StMrg
 Body         .0046     0.0 0.142 0.0167  8.5  3.2 0.55  2  0.007 0.0000     0.0 0.238
 Wing         .0086     2.5 0.430 0.0228 18.8 12.3 0.81  2  -.056 0.0000     0.0 0.244
 Strakes      .0000     5.0 0.708 0.0354 20.0 16.8 0.81  2  -.128 0.0000     0.0 0.252
 H. Tail      .0010     7.5 0.976 0.0540 18.1 17.9 0.79  2  -.209 0.0000     0.0 0.260
 V. Tail      .0012    10.0 1.237 0.0785 15.8 17.5 0.77  2  -.299 0.0000     0.0 0.268
 Canard       .0000    15.0 1.733 0.1436 12.1 15.9 0.75  2  -.501 0.0000     0.0 0.281
Interference  .0005    30.0 3.026 0.4391  6.9 12.0 0.69  2  ***** 0.0000     0.0 0.000
 Base         .0000    45.0 1.433 1.3461  1.1  1.3 0.05  3  -.887 0.0000     0.0 0.000
 Wing-Body    .0002    60.0 0.568 1.8692  0.3  0.2 0.01  3  -.894 0.0000     0.0 0.000
 Wing-Nacelle .0000    75.0 0.211 2.0429  0.1  0.0 0.00  3  -.809 0.0000     0.0 0.000
 Excressence  .0003
Wave          .0000
External      .0000                      Slope Factors
 Tanks        .0000                        Cl/Alpha (per radian)        0.0523
 Bombs        .0000                        Cdl/Cl^2                    45.6471
 Stores       .0000                      Alpha Transition Zone 2-3     38.015
 Extra        .0000
Camber        .0004                      Programmed Flap Setting           0.
_________________
Cdmin         .0163                      Flap Type        Single           1. sq. ft

Mach     =    0.17  C.G. Location =   1.6 ft, 0.20 cbar
Altitude =      0.  Reynolds Number per foot =    1.228x10^6

Parasite Drag       Induced Drag
Friction      .0154   Alpha    Cl     Cd  L/D   PF    e Zone  Cm  Cdtrim Deltrim StMrg
 Body         .0046     0.0 0.142 0.0167  8.5  3.2 0.55  2  0.007 0.0000     0.0 0.240
```

```
 Wing          .0086     2.5 0.431 0.0228 18.9 12.4 0.81  2  -.057 0.0000     0.0 0.246
 Strakes       .0000     5.0 0.709 0.0354 20.0 16.9 0.81  2  -.130 0.0000     0.0 0.253
 H. Tail       .0010     7.5 0.979 0.0542 18.1 17.9 0.79  2  -.211 0.0000     0.0 0.261
 V. Tail       .0012    10.0 1.240 0.0787 15.8 17.5 0.77  2  -.302 0.0000     0.0 0.269
 Canard        .0000    15.0 1.736 0.1437 12.1 15.9 0.75  2  -.504 0.0000     0.0 0.283
Interference   .0005    30.0 3.029 0.4388  6.9 12.0 0.69  2  ***** 0.0000     0.0 0.000
 Base          .0000    45.0 1.433 1.3468  1.1  1.3 0.05  3  -.889 0.0000     0.0 0.000
 Wing-Body     .0002    60.0 0.569 1.8696  0.3  0.2 0.01  3  -.899 0.0000     0.0 0.000
 Wing-Nacelle  .0000    75.0 0.211 2.0436  0.1  0.0 0.00  3  -.815 0.0000     0.0 0.000
 Excressence   .0003
Wave           .0000
External       .0000                       Slope Factors
 Tanks         .0000                         Cl/Alpha (per radian)        0.0526
 Bombs         .0000                         Cdl/Cl^2                    45.4682
 Stores        .0000                       Alpha Transition Zone 2-3     32.860
 Extra         .0000
Camber         .0004                       Programmed Flap Setting           0.
_________________
Cdmin          .0163                       Flap Type        Single           1. sq. ft
\
 Detailed Aerodynamics Output

 Mach     =    0.20  C.G. Location =   1.6 ft, 0.20 cbar
 Altitude =      0.  Reynolds Number per foot =    1.420x10^6

 Parasite Drag       Induced Drag
 Friction      .0154   Alpha    Cl     Cd  L/D   PF    e Zone  Cm  Cdtrim Deltrim StMrg
 Body          .0046     0.0 0.143 0.0167  8.5  3.2 0.55  2  0.007 0.0000     0.0 0.242
 Wing          .0086     2.5 0.432 0.0228 18.9 12.4 0.81  2  -.058 0.0000     0.0 0.247
 Strakes       .0000     5.0 0.712 0.0355 20.0 16.9 0.81  2  -.132 0.0000     0.0 0.255
 H. Tail       .0010     7.5 0.982 0.0543 18.1 17.9 0.79  2  -.214 0.0000     0.0 0.263
 V. Tail       .0012    10.0 1.244 0.0790 15.7 17.6 0.78  2  -.305 0.0000     0.0 0.271
 Canard        .0000    15.0 1.740 0.1440 12.1 15.9 0.75  2  -.508 0.0000     0.0 0.285
Interference   .0005    30.0 2.871 1.3064  2.2  3.7 0.20  3  -.905 0.0000     0.0 0.000
 Base          .0000    45.0 1.435 1.3489  1.1  1.3 0.05  3  -.895 0.0000     0.0 0.000
 Wing-Body     .0002    60.0 0.570 1.8704  0.3  0.2 0.01  3  -.906 0.0000     0.0 0.000
 Wing-Nacelle  .0000    75.0 0.212 2.0449  0.1  0.0 0.00  3  -.822 0.0000     0.0 0.000
 Excressence   .0003
Wave           .0000
External       .0000                       Slope Factors
 Tanks         .0000                         Cl/Alpha (per radian)        0.0529
 Bombs         .0000                         Cdl/Cl^2                    45.2499
 Stores        .0000                       Alpha Transition Zone 2-3     28.312
 Extra         .0000
Camber         .0004                       Programmed Flap Setting           0.
_________________
Cdmin          .0163                       Flap Type        Single           1. sq. ft

 Mach     =    0.25  C.G. Location =   1.6 ft, 0.20 cbar
 Altitude =      0.  Reynolds Number per foot =    1.775x10^6

 Parasite Drag       Induced Drag
 Friction      .0153   Alpha    Cl     Cd  L/D   PF    e Zone  Cm  Cdtrim Deltrim StMrg
 Body          .0046     0.0 0.143 0.0167  8.6  3.2 0.56  2  0.007 0.0000     0.0 0.245
 Wing          .0085     2.5 0.435 0.0229 19.0 12.5 0.82  2  -.060 0.0000     0.0 0.251
 Strakes       .0000     5.0 0.717 0.0357 20.1 17.0 0.81  2  -.135 0.0000     0.0 0.258
 H. Tail       .0010     7.5 0.989 0.0548 18.1 18.0 0.79  2  -.220 0.0000     0.0 0.266
 V. Tail       .0012    10.0 1.252 0.0796 15.7 17.6 0.78  2  -.312 0.0000     0.0 0.274
 Canard        .0000    15.0 1.750 0.1447 12.1 16.0 0.75  2  -.516 0.0000     0.0 0.288
Interference   .0005    30.0 2.462 1.1259  2.2  3.4 0.17  3  -.865 0.0000     0.0 0.000
 Base          .0000    45.0 1.440 1.3534  1.1  1.3 0.05  3  -.907 0.0000     0.0 0.000
 Wing-Body     .0002    60.0 0.572 1.8731  0.3  0.2 0.01  3  -.920 0.0000     0.0 0.000
 Wing-Nacelle  .0000    75.0 0.213 2.0488  0.1  0.0 0.00  3  -.838 0.0000     0.0 0.000
 Excressence   .0003
Wave           .0000
External       .0000                       Slope Factors
 Tanks         .0000                         Cl/Alpha (per radian)        0.0536
 Bombs         .0000                         Cdl/Cl^2                    44.8069
 Stores        .0000                       Alpha Transition Zone 2-3     22.463
 Extra         .0000
Camber         .0004                       Programmed Flap Setting           0.
```

```
 ________________
 Cdmin         .0163                      Flap Type        Single           1. sq. ft
\
 Detailed Aerodynamics Output

 Mach     =    0.30  C.G. Location =   1.6 ft, 0.20 cbar
 Altitude =      0.  Reynolds Number per foot =    2.130x10^6

 Parasite Drag       Induced Drag
 Friction      .0153   Alpha    Cl     Cd  L/D   PF    e Zone  Cm  Cdtrim Deltrim StMrg
  Body         .0046     0.0 0.143 0.0166  8.6  3.3 0.56  2  0.006 0.0000     0.0 0.248
  Wing         .0085     2.5 0.438 0.0229 19.1 12.7 0.82  2  -.062 0.0000     0.0 0.254
  Strakes      .0000     5.0 0.723 0.0360 20.1 17.1 0.81  2  -.139 0.0000     0.0 0.261
  H. Tail      .0010     7.5 0.998 0.0553 18.1 18.1 0.80  2  -.225 0.0000     0.0 0.269
  V. Tail      .0012    10.0 1.263 0.0803 15.7 17.7 0.78  2  -.319 0.0000     0.0 0.277
  Canard       .0000    15.0 1.764 0.1459 12.1 16.1 0.76  2  -.525 0.0000     0.0 0.291
 Interference  .0005    30.0 2.249 1.0336  2.2  3.3 0.16  3  -.849 0.0000     0.0 0.000
  Base         .0000    45.0 1.445 1.3589  1.1  1.3 0.05  3  -.920 0.0000     0.0 0.000
  Wing-Body    .0002    60.0 0.575 1.8771  0.3  0.2 0.01  3  -.935 0.0000     0.0 0.000
  Wing-Nacelle .0000    75.0 0.214 2.0541  0.1  0.0 0.00  3  -.855 0.0000     0.0 0.000
  Excressence  .0003
 Wave          .0000
 External      .0000                      Slope Factors
  Tanks        .0000                        Cl/Alpha (per radian)        0.0544
  Bombs        .0000                        Cdl/Cl^2                    44.3744
  Stores       .0000                      Alpha Transition Zone 2-3     18.541
  Extra        .0000
 Camber        .0004                      Programmed Flap Setting           0.
 ________________
 Cdmin         .0162                      Flap Type        Single           1. sq. ft

 Mach     =    0.35  C.G. Location =   1.6 ft, 0.20 cbar
 Altitude =      0.  Reynolds Number per foot =    2.484x10^6

 Parasite Drag       Induced Drag
 Friction      .0152   Alpha    Cl     Cd  L/D   PF    e Zone  Cm  Cdtrim Deltrim StMrg
  Body         .0045     0.0 0.144 0.0166  8.7  3.3 0.56  2  0.006 0.0000     0.0 0.250
  Wing         .0085     2.5 0.443 0.0230 19.3 12.8 0.82  2  -.064 0.0000     0.0 0.256
  Strakes      .0000     5.0 0.731 0.0363 20.2 17.2 0.82  2  -.144 0.0000     0.0 0.264
  H. Tail      .0010     7.5 1.009 0.0559 18.1 18.1 0.80  2  -.231 0.0000     0.0 0.272
  V. Tail      .0012    10.0 1.277 0.0813 15.7 17.7 0.79  2  -.326 0.0000     0.0 0.280
  Canard       .0000    15.0 1.783 0.1479 12.0 16.1 0.76  2  -.536 0.0000     0.0 0.294
 Interference  .0005    30.0 2.220 1.0266  2.2  3.2 0.16  3  -.857 0.0000     0.0 0.000
  Base         .0000    45.0 1.452 1.3653  1.1  1.3 0.05  3  -.934 0.0000     0.0 0.000
  Wing-Body    .0002    60.0 0.580 1.8848  0.3  0.2 0.01  3  -.954 0.0000     0.0 0.000
  Wing-Nacelle .0000    75.0 0.227 2.1039  0.1  0.1 0.00  3  -.919 0.0000     0.0 0.000
  Excressence  .0003
 Wave          .0000
 External      .0000                      Slope Factors
  Tanks        .0000                        Cl/Alpha (per radian)        0.0639
  Bombs        .0000                        Cdl/Cl^2                    40.4219
  Stores       .0000                      Alpha Transition Zone 2-3     15.720
  Extra        .0000
 Camber        .0004                      Programmed Flap Setting           0.
 ________________
 Cdmin         .0162                      Flap Type        Single           1. sq. ft
\

  Output for Module # 11
  ******************************************************************************
 SUMMARY --- ACS OUTPUT:  UAV 1

     GENERAL           FUSELAGE                          WING   HTAIL  VTAIL
 WG        255.   LENGTH           5.5   AREA           12.6    1.9    1.6
 W/S       20.3   DIAMETER         1.0   WETTED AREA    25.3    2.1    2.4
 T/W       0.00   VOLUME           3.3   SPAN           11.2    3.1    2.3
 N(Z) ULT  4.5    WETTED AREA     15.0   L.E. SWEEP      0.0    0.0    0.0
 CREW       0.    FINENESS RATIO   5.5   C/4 SWEEP      -0.6   -0.6   -0.4
 PASENGERS  0.                           ASPECT RATIO  10.00   5.00   3.50
                                         TAPER RATIO    0.80   0.90   0.90
    ENGINE             WEIGHTS           T/C ROOT       0.12   0.12   0.12
```

					T/C TIP	0.12	0.10	0.12
NUMBER	1.		W	WG	ROOT CHORD	1.2	0.7	0.7
LENGTH	1.0	STRUCT.	77.	30.1	TIP CHORD	1.0	0.6	0.6
DIAM.	0.5	PROPUL.	49.	19.4	M.A. CHORD	1.1	0.6	0.7
WEIGHT	35.2	FIX. EQ.	29.	11.2	LOC. OF L.E.	1.3	4.8	4.8
TSLS	36.	FUEL	39.	15.7				
SFCSLS	0.00	PAYLOAD	60.	23.6				
ESF	0.000	OPER IT	1.	0.4				

MISSION SUMMARY

PHASE	MACH	ALT	FUEL	TIME	DIST	L/D	THRUST	SFC	Q
TAKEOFF	0.00	0.	0.	6.0	935.6				
ACCEL	0.10	2000.	0.	0.0	0.0	19.47	71.6	0.122	13.8
CLIMB	0.14	5000.	0.	0.6	0.8	15.40	56.9	0.154	22.8
CRUISE	0.14	5000.	37.	856.6	1299.2	12.90	5.4	0.487	24.2
LANDING					537.7				

Block Time = 14.388 hr
Block Range = 1300.0 nm